(12) INTERNATIONAL APPLICATION PUBLISHED UNDER THE PATENT COOPERATION TREATY (PCT)

(19) World Intellectual Property Organization
International Bureau

(43) International Publication Date
5 October 2017 (05.10.2017)

WIPO | PCT

(10) International Publication Number
WO 2017/167360 A1

(51) International Patent Classification:
A61B 5/053 (2006.01) *A61B 5/02* (2006.01)
A61B 5/0452 (2006.01) *A61B 5/107* (2006.01)
A61B 5/042 (2006.01) *A61B 5/046* (2006.01)
A61B 5/0215 (2006.01) *A61B 5/0464* (2006.01)
A61B 5/029 (2006.01) *A61M 25/00* (2006.01)
A61N 1/05 (2006.01) *A61B 5/06* (2006.01)
A61B 5/00 (2006.01)

(21) International Application Number:
PCT/EP2016/056933

(22) International Filing Date:
30 March 2016 (30.03.2016)

(25) Filing Language: English

(26) Publication Language: English

(71) Applicants: **UNIVERSITAT POLITÈCNICA DE CATALUNYA** [ES/ES]; Jordi Girona, 31, 08034 Barcelona (ES). **FUNDACIÓ INSTITUT DE RECERCA DE L'HOSPITAL DE LA SANTA CREU I SANT PAU** [ES/ES]; C. Sant Antoni Maria Claret, 167, 08025 Barcelona (ES).

(72) Inventors: **ROSELL FERRER, Francesc Xavier**; Universitat Politècnica de Catalunya, C. Jordi Girona, 31, 08034 Barcelona (ES). **CINCA CUSCULLOLA, Juan**; Institut de Recerca del Hospital de la Santa Creu i Sant Pau, St. Antoni Maria Claret, 167, 08025 Barcelona (ES). **BRAGÓS BARDIA, Ramón**; Universitat Politècnica de Catalunya, C. Jordi Girona, 31, 08034 Barcelona (ES). **AMORÓS FIGUERAS, Gerard**; Institut de Recerca del Hospital de la Santa Creu i Sant Pau, St. Antoni Maria Claret, 167, 08025 Barcelona (ES). **JORGE VIZUETE, Esther**; Institut de Recerca del Hospital de la Santa Creu i Sant Pau, St. Antoni Maria Claret, 167, 08025 Barcelona (ES). **GARCÍA SÁNCHEZ, Tomàs**; Universitat Politècnica de Catalunya, C. Jordi Girona, 31, 08034 Barcelona (ES). **SÁNCHEZ TERRONES, Benjamín**; Universitat Politècnica de Catalunya, C. Jordi Girona, 31, 08034 Barcelona (ES).

(74) Agent: **ZBM PATENTS - ZEA, BARLOCCI & MARKVARDSEN**; Pl. Catalunya, 1 2nd floor, 08002 Barcelona (ES).

(81) Designated States *(unless otherwise indicated, for every kind of national protection available)*: AE, AG, AL, AM, AO, AT, AU, AZ, BA, BB, BG, BH, BN, BR, BW, BY, BZ, CA, CH, CL, CN, CO, CR, CU, CZ, DE, DK, DM, DO, DZ, EC, EE, EG, ES, FI, GB, GD, GE, GH, GM, GT, HN, HR, HU, ID, IL, IN, IR, IS, JP, KE, KG, KN, KP, KR, KZ, LA, LC, LK, LR, LS, LU, LY, MA, MD, ME, MG, MK, MN, MW, MX, MY, MZ, NA, NG, NI, NO, NZ, OM, PA, PE, PG, PH, PL, PT, QA, RO, RS, RU, RW, SA, SC, SD, SE, SG, SK, SL, SM, ST, SV, SY, TH, TJ, TM, TN, TR, TT, TZ, UA, UG, US, UZ, VC, VN, ZA, ZM, ZW.

(84) Designated States *(unless otherwise indicated, for every kind of regional protection available)*: ARIPO (BW, GH, GM, KE, LR, LS, MW, MZ, NA, RW, SD, SL, ST, SZ, TZ, UG, ZM, ZW), Eurasian (AM, AZ, BY, KG, KZ, RU, TJ, TM), European (AL, AT, BE, BG, CH, CY, CZ, DE, DK, EE, ES, FI, FR, GB, GR, HR, HU, IE, IS, IT, LT, LU, LV, MC, MK, MT, NL, NO, PL, PT, RO, RS, SE, SI, SK, SM, TR), OAPI (BF, BJ, CF, CG, CI, CM, GA, GN, GQ, GW, KM, ML, MR, NE, SN, TD, TG).

Declarations under Rule 4.17:

— *as to applicant's entitlement to apply for and be granted a patent (Rule 4.17(ii))*

Published:

— *with international search report (Art. 21(3))*

WO 2017/167360 A1

(54) **Title**: SYSTEMS AND METHODS TO ASSESS INFARCTED MYOCARDIAL TISSUE BY MEASURING ELECTRICAL IMPEDANCE DURING THE CARDIAC CYCLE

(57) **Abstract**: Disclosed herein are methods and devices used to recognize the extent and deepness of infarcted tissue, such as chronic myocardial infarcted tissue. The invention applies to the heart tissue, but can also be used to assess cicatricial processes in other organs. Examples of the method comprise injecting pulses of alternating current at a broadband of frequencies while measuring the voltage signal continuously (at a very high sampling rate) to obtain the electrical impedance (Z(f,t)) during the entire cardiac cycle. The impedance measurements may be taken using an intracavitary electrocatheter.

SYSTEMS AND METHODS TO ASSESS INFARCTED MYOCARDIAL TISSUE BY MEASURING ELECTRICAL IMPEDANCE DURING THE CARDIAC CYCLE

The present disclosure relates to methods and devices to assess infarcted tissue by measuring electrical impedance. More specifically, the methods and devices may be used to recognize the extent and deepness of an infarcted tissue, such as for example myocardial infarcted tissue.

BACKGROUND ART

Ventricular arrhythmias are responsible of approximately 60% of sudden deaths in patients with a previously cardiac infarction. Radiofrequency ablation of the arrhythmogenic foci is able to treat around 50-80% of the patients with postinfarction ventricular arrhythmias. The success rate of this procedure could be increased by improvements in the identification and localization of the arrhythmogenic foci in the clinical practice. The clinical intracardiac navigation systems used nowadays (for example: (i) CARTO®, provided by Biosence Webster®, (ii) NavX™, provided by St. Jude Medical™ , or (iii) Rhythmia™, provided by Boston Scientific™) locate the postinfarction scar by local measures of voltage using intracavitary electrocatheters. A major drawback of the voltage measurements is that they cannot determine if the scar is completely transmural or not. Another drawback is that these voltage measurements depend on the wave front activation pattern, that can change if the patient suffers and ectopic arrhythmic episode.

The characterization of biological substrates by means of electrical impedance provides relevant physiological information about the pathological status of the tissues. It has been reported that normal and infarcted myocardium can be recognized by measuring the myocardial electrical impedance (module and phase angle) using an intracardiac electrocatheter, see e.g. “Warren M, et al. Percutaneous electrocatheter technique for on-line detection of healed transmural myocardial infarction. Pacing Clin Electrophysiol. 2000;23:1283–1287” (*Warren 2000”*). As compared with the normal myocardium, the necrotic infarct scar shows a lower impedance module and a flat phase angle deviation. Measuring the electrical

impedance as an indicator of the structural condition of the cardiac tissue has been already proposed in the past. Previous documents (US5494042A; US2001018608A; US5485849) have described systems and methods using the impedance to identify infarcted regions of heart. However, these systems measure the impedance at a single frequency or at few selected frequencies (between 5 Hz and 50 kHz). With these "old" techniques, only few impedance measurements could be taken during the cardiac cycle due to the time required to inject the wide current spectrum by frequency sweeping. The cardiac movement during contraction and relaxation induces impedance changes that increase the dispersion of impedance measures and this curtails the capacity of the system to recognize the structural derangement.

It is also noted that prompt coronary artery reperfusion in patients with acute myocardial infarction favors cell survival and ultimately promotes the development of heterogeneous transmural infarct scar (see Francone M., et al. Impact of primary coronary angioplasty delay on myocardial salvage, infarct size, and microvascular damage in patients with ST-segment elevation myocardial infarction. Insight from cardiovascular magnetic resonance. J. Am. Coll. Cardiol. 2009;54:2145–2153). The interspaced islands of surviving myocytes may act as slow conducting pathways thereby favoring re-entrant arrhythmias (Arenal A et al. Tachycardia-related channel in the scar tissue in patients with sustained monomorphic ventricular tachycardias: Influence of the voltage scar definition. Circulation 2004;110:2568–2574.; Nakahara S., et al. Characterization of the arrhythmogenic substrate in ischemic and nonischemic cardiomyopathy. Implications for catheter ablation of hemodynamically unstable ventricular tachycardia. J. Am. Coll. Cardiol. Elsevier Inc.; 2010;55:2355–2365) and increasing mortality (Yan A.T., et al. Characterization of the peri-infarct zone by contrast-enhanced cardiac magnetic resonance imaging is a powerful predictor of post-myocardial infarction mortality. Circulation 2006;114:32–39). Postinfarction ventricular arrhythmias can be suppressed by electrical catheter ablation of the arrhythmogenic substrate but this procedure requires an accurate delineation of the infarct scar and a precise location of the target ablation sites scattered within the infarcted region. The cardiac navigation systems employed in the catheter ablation procedures utilize the mapping of low voltage endocardial

electrograms to delineate the borders of the infarct scar although this technique does not allow appropriate discrimination among sites with different degrees of transmural involvement (Codreanu A., et al. Electroanatomic characterization of post-infarct scars. Comparison with 3-Dimensional myocardial scar reconstruction based on magnetic resonance imaging. J. Am. Coll. Cardiol. 2008;52:839–842).

In clinical practice, the heterogeneous nature of the infarct scar may only be assessed accurately by cardiac magnetic resonance imaging (Klein C., et al. Assessment of myocardial viability with contrast-enhanced magnetic resonance imaging: comparison with positron emission tomography. 2002;105:162–167), but previous studies have reported differential biophysical electrical characteristics between the normal myocardium and the infarcted tissue (Warren 2000). Myocardial electrical impedance is a biophysical property of the heart that is influenced by the intrinsic structural characteristics of the myocardial tissue (Sperelakis N., et al. Electrical impedance of cardiac muscle. Circ. Res. 1961;9:1280–1283) as denoted by experimental models of acute and chronic myocardial infarction (Cinca J., et al. Passive transmission of ischemic ST segment changes in low electrical resistance myocardial infarct scar in the pig. Cardiovasc. Res. 1998;40:103–112 ; Fallert MA et al. Myocardial electrical impedance mapping of ischemic sheep hearts and healing aneurysms. Circulation 1993;87:199–207; Salazar Y et al. Transmural versus nontransmural in situ electrical impedance spectrum for healthy, ischemic, and healed myocardium. IEEE Trans. Biomed. Eng. 2004;51:1421–1427). In “Sanchez B et al. A new measuring and identification approach for time-varying bioimpedance using multisine electrical impedance spectroscopy. Physiol. Meas. 2013;34:339–57” a refinement of the impedance measurement technique was demonstrated by applying fast broadband electrical impedance spectroscopy (EIS) that permitted to characterize the changes in myocardial impedance during the cardiac cycle in normal and acute ischemic conditions in the in situ porcine heart (Jorge E., et al. Early detection of acute transmural myocardial ischemia by the phasic systolic- diastolic changes of local tissue electrical impedance. Am. J. Physiol. Heart Circ. Physiol. 2015;310:H436–H443).

SUMMARY OF THE INVENTION

The aim of the present invention is to provide a measuring device for medical applications, which can be used to characterize tissues, for example myocardial tissue structure integrity and solve at least partly the drawbacks and limitations of known systems used in clinical practice. This is achieved by measuring the changes in impedance during the entire cardiac cycle by injecting electrical current with a broadband spectrum.

A further capability of the present invention is to analyze the changes in myocardial impedance during the cardiac cycle in an infarct scar to detect heterogeneous transmural involvement in the infarcted region.

The present invention takes benefit of the measurements of electrical resistivity of heart tissue using the novel technique of fast broadband electrical impedance spectroscopy (EIS) (see “Sanchez B., et al. A new measuring and identification approach for time-varying bioimpedance using multisine electrical impedance spectroscopy. Physiol. Meas. 2013;34:339–57”). This new technique enables time-varying bioimpedance measurements within the entire cardiac cycle, at simultaneous multiple frequencies (between 1 kHz - 1 MHz), obtaining up to 1,000 spectrum measures/sec. With this new procedure it is possible to record the phasic systolic and diastolic changes in myocardial impedance elicited during the cardiac cycle so the movement-induced impedance changes become useful and gives additional information. This increases the accuracy of the technique because it provides more information about the tissue characteristics.

It is proposed to use this new system and method to recognize the extent and deepness of infarcted tissue by measuring electrical impedance, for example the extent and deepness of chronic myocardial infarcted tissue by measuring the myocardial electrical impedance during the entire cardiac cycle using one or more intracavitary electrocatheters.

The system and method may be used to assess the extent and deepness of chronic myocardial infarcted tissue by measuring systolic and diastolic myocardial electrical impedance.

The invention applies specifically to the heart tissue, but can also be used to assess fibrotic processes in other organs.

In a first aspect a method of assessing a cardiac tissue is disclosed. The method comprises selecting an area of interest of the cardiac tissue; identifying one or more measurement locations in the selected area of interest; placing an electrocatheter probe at the one or more measurement locations; providing a broadband spectrum signal to the one or more measurement locations using the electrocatheter probe; identifying a diastolic phase of the cardiac cycle; measuring impedance of the cardiac tissue during the identified diastolic phase; identifying a systolic phase of the cardiac cycle ; measuring impedance of the cardiac tissue during the identified systolic phase; and assessing said cardiac tissue based on said diastolic and systolic impedance measurements.

Embodiments of the inventive method comprise injecting current pulses with a broadband spectrum while measuring the voltage signal continuously (at a sampling rate higher than the maximum spectral component and in the order of ten to a few hundred pulses during a cardiac cycle) to obtain the electrical impedance (Z(f,t)) during the entire cardiac cycle. According to examples of the invention, the impedance measurements are taken using an intracavitary electrocatheter with at least one electrode placed at the tip of the catheter and a skin electrode or another electrocatheter inside the body.

In another aspect, a device is disclosed. The device comprises means for selecting an area of interest of a cardiac tissue; means for identifying one or more measurement locations in the selected area of interest; means for placing an electrocatheter probe at the one or more measurement locations; means for providing a broadband signal to the one or more measurement locations using the electrocatheter probe; means for identifying a diastolic phase of the cardiac cycle; means for measuring impedance of the myocardial tissue during the identified diastolic phase; means for identifying a systolic phase of the cardiac cycle; means for measuring impedance of the cardiac tissue during the identified systolic phase; and means for assessing said cardiac tissue based on said diastolic and systolic impedance measurements.

Another aspect of the present invention relates to a device. The device comprises an arbitrary waveform generator (AWG) to deliver one or more broadband frequency current signals having an amplitude and a duration lasting over a time period associated with one or more cardiac cycles. The device further comprises a multielectrode probe, coupled to the AWG, configured to apply the broadband frequency current signals in vivo to a cardiac tissue and measure impedance of the cardiac tissue. The device further comprises an acquisition module (AM). The AM comprises an electrocardiograph (ECG) recorder and may comprise a blood pressure recorder. The device further comprises a controller coupled to the AWG and to the AM and configured to receive the impedance measurements during the duration of the broadband signal, to receive the recordings of the acquisition module during the duration of the broadband signal, to identify a systolic or diastolic phase of a cardiac cycle, to correlate the impedance measurements with the identified phase of the cardiac cycle, and to identify the cardiac tissue as transmural or non-transmural in response to said correlation.

Embodiments of the present invention relate to a device and method for mapping the inner (endocardial) regions of the heart, for example an atrial region or a ventricular region, to delineate the extent of necrotic scar. This may be done by measuring the electrical impedance during the entire cardiac cycle after injecting current pulses at multiple frequencies simultaneously. That has a clinical application in the catheter ablation treatment of ventricular arrhythmias in patients with myocardial infarction.

Some advantages of the equipment according to embodiments of the invention may be:

- Unlike other impedance mapping techniques, the present invention is based on simultaneous impedance measurements performed at multiple frequencies, e.g. using electrical impedance spectroscopy (EIS), providing more information about the structural condition of the myocardium tissue. Additionally, these simultaneous multifrequency measurements are performed in a relatively short time compared to the cardiac cycle (in the range of 1 ms, for example between 0.1 and 10 ms, or for example between 0.5 and 2 ms) thus allowing to

acquire the whole time-frequency information into the cardiac cycle. In this way, the impedance spectrum measurements are performed at known moments of the cardiac cycle eliminating the influence of the myocardium movement. This new device and method allow a more accurate recognition of the extent and transmurality of the infarct scar and permit a better identification of the target sites for electrical ablation of ventricular arrhythmias.

- Unlike the voltage mapping, the impedance mapping is not influenced by the direction of the activation wave front and because of that, it does not require reassessment of the map data whenever an ectopic rhythm supervened during the clinical procedure.

- Unlike the voltage mapping, the impedance mapping can detect the subendocardial, subepicardial and midmyocardial degree of fibrosis. Therefore the impedance mapping can detect if the fibrosis is transmural or non-transmural.

In yet a further aspect, a system is disclosed. The system comprises a device according to previous aspects disclosed herein, and an external processing apparatus. The external processing apparatus is connectable to the device via a communication link. The external processing apparatus is configured to run an application to determine the suitable waveform to be uploaded in the AWG, the acquisition strategy, and to apply the algorithms to obtain values of the tissue state estimators from the time-frequency characteristics of the measured impedance signals.

In yet a further aspect, a controller is disclosed. The controller comprises a signal selector module, configured to be coupled to an arbitrary waveform generator (AWG), to provide to the AWG parameters of a broadband current pulse signal to be applied on a cardiac tissue. The controller further comprises a receiver configured to be coupled to an acquisition module to receive impedance measurements and ECG and blood pressure recordings from the acquisition module. The controller further comprises a processing module, configured to identify a systolic and/or diastolic phase of the cardiac cycle as a function of said received recordings. Furthermore, the controller comprises an assessment module,

configured to identify a state of the cardiac tissue as a function of the impedance measurements and the identified phase.

In another aspect, a computer program product is disclosed. The computer program product may comprise program instructions for causing a computing system to perform a method of assessing cardiac tissue according to some examples disclosed herein. The computer program may merge the results obtained with the impedance map with the results obtained with the voltage mapping.

The computer program product may be embodied on a storage medium (for example, a CD-ROM, a DVD, a USB drive, on a computer memory or on a read-only memory) or carried on a carrier signal (for example, on an electrical or optical carrier signal).

The computer program may be in the form of source code, object code, a code intermediate source and object code such as in partially compiled form, or in any other form suitable for use in the implementation of the processes. The carrier may be any entity or device capable of carrying the computer program.

For example, the carrier may comprise a storage medium, such as a ROM, for example a CD ROM or a semiconductor ROM, or a magnetic recording medium, for example a hard disk. Further, the carrier may be a transmissible carrier such as an electrical or optical signal, which may be conveyed via electrical or optical cable or by radio or other means.

When the computer program is embodied in a signal that may be conveyed directly by a cable or other device or means, the carrier may be constituted by such cable or other device or means.

Alternatively, the carrier may be an integrated circuit in which the computer program is embedded, the integrated circuit being adapted for performing, or for use in the performance of, the relevant methods.

BRIEF DESCRIPTION OF THE DRAWINGS

Particular embodiments of the present invention will be described in the following by way of non-limiting examples, with reference to the appended drawings, in which:

FIG. 1 is a schematic representation of the system used to record simultaneously the phasic changes of myocardial electrical impedance, left ventricular (LV) pressure and surface ECG;

FIG. 1B schematically illustrates various example electrocatheter configurations;

FIG. 2 is a representation of the (non-)periodic broadband EIS for the nonparametric-in-time measurement of the time-varying bioimpedance;

FIG. 3 displays an example of a multisine signal and its spectrum;

FIG. 4A represents a resistivity spectrum which has a modulation due to myocardium movement;

FIG. 4B represents the modulation of the resistivity waveform due to myocardium movement;

FIG. 5 is a Wessel plane showing a set of arcs corresponding to several cardiac cycles;

FIG. 6A represents the time course of R0, R∞ obtained by acquiring 60 spectra per second and fitting them to the Cole model for impedance;

FIG. 6B represents the time course of α obtained by acquiring 60 spectra per second and fitting them to the Cole model for impedance;

FIG. 6C represents the time course of fc obtained by acquiring 60 spectra per second and fitting them to the Cole model for impedance;

FIG. 7 is a flow diagram of a method of assessing a cardiac tissue;

FIG.7A displays impedance spectra of three regions with three tissue states and their modulation range due to myocardium movement in the three tissue states;

FIG. 7B shows the arcs in the Wessel plane for the three regions.

FIG. 8 shows the time-domain of impedance magnitude at a selected frequency (1 kHz) of 4 different tissues states;

FIG. 9 shows magnitude of the normal (NZ), border (BZ) and healed-scar (infarcted, IZ) zones impedance time signal at three different frequencies (1 kHz, 307 kHz and 939 kHz);

FIG.10 shows the corresponding phase angle at the same frequencies as the ones indicated in FIG. 9;

FIG.11 represents the resistivity time course at a frequency of 1 kHz, for two tissue state (normal and acute ischemic) together with the synchronously acquired ventricle pressure, its derivative and the ECG;

FIG.12A represents the resistivity at a given frequency (top) and the left ventricular pressure (LVP) (bottom);

FIG. 12B shows the cycle described by the evolution of the signal in the Resistivity-LVP plane;

FIG. 13A shows the Resistivity-LVP loop at baseline and after 30 min. of left anterior descending (LAD) coronary artery occlusion;

FIG. 13B shows the Resistivity-LVP loop area mean at different frequencies at baseline and after 30 minutes of ischemia;

FIG. 14 shows the Resistivity-LVP loop for four different tissue-states;

FIG. 15 illustrates a schematic representation of a heart with two electrocatheters;

FIG. 16A illustrates the mean value of resistivity (top) and phase angle (bottom) vs. the excitation frequency for three different tissues: healthy tissue (N), non-transmural and transmural infarcted scar (ISN and IST, respectively);

FIG. 16B illustrates the mean values of resistivity (top) and phase angle (bottom) at 4 selected frequencies (1, 41, 307 and 1000 kHz) for the three tissue;

FIG. 17 illustrates a linear correlation between myocardial resistivity (upper-left) / phase angle (lower-left) and the percentage of fibrosis;

FIG. 18 illustrates the comparative pattern of the Cole impedance model obtained in normal (N: white), non-transmural scar (ISN: grey) and infarcted transmural scar (IST: black);

FIG. 19A illustrates myocardial tissue electrical resistivity and ECG in a normal myocardium;

FIG. 19B illustrates myocardial tissue electrical resistivity and ECG in a non-transmural infarct scar;

FIG. 19C illustrates myocardial tissue electrical resistivity and ECG in a transmural infarct scar;

FIG. 20 is a multiparametric analysis showing that a combination of resistivity and fc improve the predictive ability to discriminate between both fibrotic tissues.

DETAILED DESCRIPTION OF EXAMPLES

Non-limiting examples of the present disclosure will be described in the following, with reference to the appended drawings.

Examples of the present invention provide a system of monitoring myocardial tissue that comprises:

- At least one contact electrode on the body; and

- At least one electrode placed at the tip of an electrocatheter to be inserted through blood vessels or body openings.

The steps comprised to perform an impedance measurement using this system may be:

1- Generate and apply to the patient an alternating broadband electrical current signal through the electrodes of an intracavitary electrocatheter, between an electrode of an intracavitary electrocatheter and an external skin electrode or between electrodes placed in two different electrocatheters.

2- Measure the voltage signals across a given pair of electrodes of the electrocatheter or / and between an electrode of an intracavitary electrocatheter and an external skin electrode.

3- Determine the impedance at each frequency and fit the values to a custom mathematical model.

4- The fitted parameters are the inputs of an algorithm that outputs a numerical value directly related to the tissue structural integrity. This algorithm may take into account:

- The values and the absolute or relative changes in impedance or admittance magnitude or phase angle (or alternative representations as real and imaginary part of impedance or admittance, or as intrinsic parameters, resistivity, conductivity and permittivity) or in the impedance or admittance model parameters in selected points of the cardiac cycle. In a preferred case, in the systolic and diastolic points determined by synchronism with other physiological signals (ECG, arterial or left ventricular pressure), or in the maximum and minimum of impedance or admittance related signals.
- The shape (slope in selected points, number and type of local maxima and minima, spectral content) of impedance magnitude or phase angle, or their alternative representations as real and imaginary parts, or in the signals corresponding to the time evolution of the impedance model parameters.
- The ratios, differences, areas determined by the aforementioned signals at different frequencies or model parameters or the combination between them and other physiological signals (ECG, arterial or left ventricular pressure).

Apparatus and method description

FIG. 1 is a schematic representation of the system used to record simultaneously the phasic changes of myocardial electrical impedance, left ventricular (LV) pressure and surface ECG. Electrical impedance at a myocardium 50 was

measured, using a four electrode electrocatheter 105, by applying an alternating current between the outer pair of electrodes (105a, 105d), while the inner two electrodes (105b, 105c) were employed to measure the resulting potential difference. AFE: analog front-end.

The apparatus is made up the following blocks (**FIG 1**):

1. A main block that comprises an arbitrary waveform generator 110 (AWG-Signal generator) that generates the waveform of the signal to be injected to the myocardium and a digitizer 115 that acquires the signals coming from the front-end (AFE). It also takes care of the synchronism between generation and acquisition. The main block includes a processor to control the sequence of operations.
2. A front-end block 120 that adapts the signal from the AWG-Signal generator 110 to a voltage or current range that fits the electrical safety standards and minimizes the effect of the electrode-tissue impedance. It also includes one or several voltage detection channels to amplify the voltage signals in the catheter and skin electrodes also minimizing the effect of the electrode-tissue impedance. It can also detect and amplify differences between these voltages. A channel to measure the injected current can also be included. The front-end can be adapted to several electrode configurations (2, 3 and 4 electrode configurations) and even switch between them. In cases where more than four electrodes (including skin or electrocatheter electrodes) are used, the frond-end can also select the most appropriate electrodes to inject or detect the signals.
3. A set of electrodes (105a, 105b, 105c, 105d) placed in the tip of a catheter and in the surface of the subject. Preferred electrode combinations can be, for example:
    - 2 electrodes: one in the catheter tip and one external, in the subject surface
    - 2 electrodes: one in the catheter tip and one annular near the catheter tip

- 3 electrodes: one in the catheter tip, one annular near the catheter tip and one external, in the subject surface.
- 4 electrodes: one in the catheter tip, one annular near the catheter tip and two external, in the subject surface.
- 2, 3 or 4 electrode technique using two different catheters in different locations of the heart.

4. Additional channels or connection to additional measurement systems if integrated in a higher level apparatus, to acquire ECG, pressure and/or flux signals synchronously with the impedance acquisitions
5. A computer or external processor 130 connected to the apparatus 100 controller through a communication link, running an application that determines the suitable waveform to be uploaded in the AWG 110, the acquisition strategy, that applies the algorithms to obtain the values of the tissue state estimators from the time-frequency characteristics of the measured impedance signals and creates and displays a map of tissue properties that could be merged with the voltage mapping.

FIG. 1B schematically illustrates various electrocatheter configurations A-E that may be used alternatively. Electrocatheter A comprises a body 21A, an electrode 22A and ring electrodes 23A and 24A. Electrode 22A may be used for measuring impedance and/or for ablation purposes. The ring electrodes may be used to detect voltage or to inject current. Electrocatheter B may comprise a body 21B, an electrode 22B and ring electrodes 23B and 24B. Electrode 22A may be smaller than the one used in electrocatheter A and may be used for measuring voltage or for injecting current. The ring electrodes may be used, as previously, to detect voltage or to inject current. Electrocatheter C may be similar to electrocatheter B. It may comprise a body 21C, an electrode 22C and ring electrodes 23C and 24C. However, electrode 22C may be to a lateral position and not at the tip of body 21C and may also be used for measuring impedance or for injecting current. The ring electrodes may be used, as previously, to detect impedance or to inject current. Electrocatheter D may comprise a body 21D, an electrode 22D at the tip of the body 21D, ring electrodes 23D and 24D and a lateral electrode 25D. Electrode 22D may be used for ablation whereas electrode 25D may be used for measuring

voltage or for injecting current. The ring electrodes may be used, as previously, to detect voltage or to inject current. Electrocatheter E may comprise a body 21E, one or more ring electrodes 23E and an array of four lateral electrodes 25E, 26E, 27E and 28E. The lateral electrodes may be used for injection or voltage detection and measurement whereas the ring electrodes may be used, as previously, to detect voltage or to inject current, accordingly. Alternatively, the array of four lateral electrodes may comprise a mechanism to separate them from the catheter surface so that they may contact the myocardium tissue without the catheter body coming in contact with the tissue. In another alternative embodiment, the array of four electrodes may be arranged around the tip of the catheter. Another alternative is to use a catheter with many electrodes, for example over an almost cylindrical surface that may be inflated against the surface of a cardiac chamber and to take measurements between selectable electrodes.

Instead of using a sequence of sinusoidal signals, whose frequency is swept then acquiring information about the impedance at different frequencies in different parts of the cardiac cycle, the fast broadband EIS methods injects bursts or a continuous periodic signal that contains a set of measurement frequencies simultaneously. The minimum length of this signal is one period of the slowest frequency. That is, in a typical case, 1 ms for a minimum frequency of 1 kHz. This would allow acquiring a maximum of 1000 whole impedance spectra per second. Nevertheless, this is usually not needed and a few tenths of spectra per second are enough. The most important is, however, the fact that the acquisition of the resulting voltage and current signals only takes 1 ms, then acquiring a quasi-static picture of the tissue state in a given point of the cardiac cycle. **FIG. 2** describes this acquisition method. The voltage and current bursts are drawn longer that they can be for clarity. They can be as short as $1/1000^{th}$ of the approximate cycle period.

FIG. 2 is a representation of the (non-)periodic broadband EIS for the nonparametric-in-time measurement of the time-varying bioimpedance $Z(\omega k,t)$, with ωk being the excitation (angular) frequency. Two possible approaches exist, where the bio-system is excited either (A) with a continuous reference broadband signal r(t)or (B) with a non-continuous one. (see “Sanchez B et al. A new measuring and

identification approach for time-varying bioimpedance using multisine electrical impedance spectroscopy. Physiol Meas. 2013;34:339–57").

There is a variety of signals that allow acquiring a whole spectrum in a given bandwidth: filtered noise, pseudo-random pulse sequences, Discrete Interval Binary Sequences, chirp signals and multisine or multitone signals. This last type of signals, which consist in the addition of a given number of sinusoidal signals, is preferred for our usage because it applies the minimum amount of energy to the tissue given that they only have energy in the selected frequency samples. In other words, for a given energy limit of the injected signal, due to electrical safety reasons, the components of the multisine can have more amplitude than other signals, then allowing to reach a higher signal to noise ratio and then a higher accuracy in the spectrum estimation at the selected frequencies.

FIG. 3 displays an example of multisine signal and its spectrum. The amplitudes and frequencies can be distributed to reach an optimal adaptation to the expected impedance spectrum and there are several methods to distribute the phase of the multisine components in order to reach a minimum amplitude, for a given RMS signal value given by the amount of frequency components and their corresponding amplitudes. This is usually referred as obtaining a minimal Crest Factor (the ratio between the peak amplitude and the RMS value. Crest factors in the range of 1.5 to 3 can be obtained for multisines with 20-25 components.

With the described apparatus, method and signal, we are able of obtaining any time-frequency impedance feature in the 1 kHz – 1 MHz range and for the times involved in the dynamic behavior of the beating heart.

FIG. 4A summarizes this by representing a resistivity spectrum which has a modulation due to myocardium movement, but being now this modulation a source of information, given that the waveform of the impedance as a function of time can be determined at every measured frequency (41 kHz for example in the figure).

FIG. 4B represents the modulation of the resistivity waveform due to myocardium movement. It shows the time course of the impedance as a function of time, represented for all 26 measured frequencies. The mean value clearly changes, but

also the signal shapes may change from low frequencies to high frequencies, and may change in a different way if there is a pathology.

If the signals are acquired with enough quality and there is a suitable calibration method to correct the errors induced by electrodes, cables and the acquisition system frequency response, the acquired spectra can be fitted to one or several curves that follow the Cole model and then be parametrized by four parameters. The equation for the impedance representation is the following one:

$$Z(f) = R_\infty + \frac{R_0 - R_\infty}{1 + \left(j\frac{f}{f_c}\right)^\alpha}$$ **Equation 1**. Cole model

The parameter R_0 provides information on the extracellular space while R_∞ depends on the total volume and the ratio between them on the cell density. The central relaxation frequency f_c depends on the average cell size and the parameter α is related to the cell shape and size homogeneity. That means that structural information about the tissue can be obtained from the spectra obtained at every cycle point. If represented in the Wessel plane, the impedance spectra of impedance relaxations of biological materials describe circumference arcs.

FIG. 5 (Wessel plane) displays the set of arcs corresponding to several cardiac cycles.

FIG. 6A represents the time course of R_0, R_∞, **FIG. 6B** the time course of α and **FIG. 6C** the time course of f_c obtained by acquiring 60 spectra per second and fitting them to the Cole model for impedance.

Summarizing, with the presented combination of apparatus, acquisition method and signal, it is possible to place a catheter in a given point of the myocardium and, in the time corresponding to a beat cycle, acquire an amount of impedance spectra able to characterize the tissue including time and frequency information, then allowing a better characterization that would help identifying the tissue structural integrity in endocardial or epicardial mapping procedures. This should improve the detection of the areas with non-transmural infarction, which could be arrhythmia

foci, in the catheter ablation treatment of malignant ventricular arrhythmias in patients with myocardial infarction.

FIG. 7 is a flow diagram of a method of assessing a cardiac tissue. In a first block 705, an area of interest of the cardiac tissue is selected. Then, in block 710, one or more measurement locations in the selected area of interest are identified. In block 715, an electrocatheter probe at the one or more measurement locations is placed. In block 720, a broadband spectrum signal is provided to the one or more measurement locations using the electrocatheter probe. In block 725, a diastolic phase of the cardiac cycle is identified. In block 730 the impedance of the cardiac tissue is measured during the identified diastolic phase. In block 735, a systolic phase of the cardiac cycle is identified. In block 740 impedance of the cardiac tissue is measured during the identified systolic phase. Finally, in block 745, the cardiac tissue is assessed and displayed based on the diastolic and systolic phase impedance measurements.

In the following figures, several examples of signals that can be used to derive estimators of the myocardial state are shown.

FIG.7A displays impedance spectra of three tissue states and their modulation range due to myocardium movement in three tissue states, characterized by their fibrosis percentage: normal tissue (2% fibrosis), healed scar (84% fibrosis) and border zone (53% fibrosis).

FIG. 7B shows the arcs in the Wessel plane for the three regions. It can be seen how normal tissue has higher impedance while healed scar has not only lower average impedance but also lower modulation and an almost flat spectrum, revealing its resistive behaviour due to the absence of viable cells. Border zone is similar to the non-transmural infarction areas that can be foci of arrhythmia.

FIG. 8 shows the time-domain of impedance magnitude at a selected frequency (1 kHz) of 4 different tissues states. In this case, also an acute ischemic area is included. It can be seen how the different tissue-state areas provide not only different average impedance values, but also different modulations and different signal shapes

FIG. 9 shows magnitude of the normal (NZ), border (BZ) and healed-scar (infarcted, IZ) zones impedance time signal at three different frequencies (1 kHz, 307 kHz and 939 kHz).

FIG. 10 shows the corresponding phase angle at the same frequencies as the ones indicated in **FIG. 9**. It can be seen how not only the average value, modulation and signal shape (slope, symmetry, number of local maxima and minima, complexity (spectral content), but also how these features change with frequency. Therefore it is possible to define estimators with more information content and more ability to separate measures using the combined time and frequency content.

Up to the extent of what has been described, the variables involved in the definition of estimators of the tissue state can be not only impedance but also admittance or the related intrinsic parameters, resistivity, conductivity and permittivity. For all of them, the estimators can take into account the values and the absolute or relative changes of the magnitude or phase angle or their alternative representations as real and imaginary part. It can also take into account the model parameters after fitting any of the aforementioned variables spectrum to a mathematical model. Their time course or their values in selected points of the cardiac cycle. In a preferred case, in the systolic and diastolic points determined by synchronism with other physiological signals (ECG, arterial or left ventricular pressure), or in the maximum and minimum of impedance or admittance related signals. Information can also be contained in the delay respect these signals.

FIG.11 represents the resistivity time course at a frequency of 1 kHz, for two tissue state (normal and acute ischemic) together with the synchronously acquired ventricle pressure, its derivative and the ECG.

Additionally to the possible definition of pathology-dependent delays between the reference signals (ECG, arterial or left ventricular pressure) and the impedance signals, there is a specific representation that gives information about the work performed by the myocardium section that is being measured, and that, consequently, will change depending on the tissue state.

This is represented in **FIG. 12A** and **FIG. 12B**. **FIG. 12A** represents the resistivity at a given frequency (top) and the left ventricular pressure (LVP) (bottom). In **FIG. 12B**, the cycle described by the evolution of the signal in the Resistivity-LVP plane is shown. This should not be mistaken with the well-known Pressure-Volume diagram, whose area represents the work performed by the whole ventricle. In this case we are representing for the first time a figure whose cycle follows the evolution of a global ventricle variable (the pressure) and the impedance in a localized point. Being the impedance dependent on the myocardium movement in that point, the area of the figure would depend on the work performed by that part of the myocardium. Then it would allow distinguishing active regions (those where the cells contraction provokes the pressure change and where the cells contraction precedes the pressure rise from passive zones, those where tissue deformation is consequence of the pressure change and where both changes are in-phase.

Figures 13A and **13B** respectively show the Resistivity-LVP loop at baseline and after 30 min. of left anterior descending (LAD) coronary artery occlusion, and the Resistivity-LVP loop area mean at different frequencies at baseline and after 30 minutes of ischemia. The figures show how the area of the Resistivity-LVP loop is reduced after 30 minutes of acute ischemia compared to its baseline value. Both tissues have mobility, but the ischemic one is following passively the movement induced by the pressure, showing the impedance less delay respect to the pressure and being the Resistivity -LVP diagram near to a line, then having less area. **FIG. 13B** shows how the separation between both tissue states is better at a given frequency, then having again the time-frequency impedance acquisition an added value.

FIG. 14 shows the Resistivity-LVP loop for four different tissue-states. The healed scar not only has lower resistivity but also shows almost no area because it follows the movement passively, then in-phase with the LV pressure. The border-zone, our detection target, has a smaller impedance and impedance modulation that the normal (basal) tissue, but, still having active myocytes, it performs work and shows higher area value.

The obvious fact that the impedance changes are related not only with the tissue state but with the motility can be corroborated by applying drugs that affect motility without destroying the cells.

Myocardial healthy tissue, non-transmural infarct zones and transmural infarct zones can be recognized *in vivo* by specific changes of their myocardial electrical impedance. Myocardial impedance mapping can identify the degree of fibrosis, and therefore the extent and transmurality of the infarct scar. This technique may improve the yielding of catheter ablation of ventricular arrhythmias in patients with chronic myocardial infarction.

FIG. 15 illustrates a schematic representation of a heart with two electrocatheters; one in the left ventricle 135 and one in the right ventricle 140. The grey area in between the catheters 145 represents an infarct scar in the mid-cardiac septum that could not be detected using the measure of voltage but that can be detected by the impedance spectroscopy measurements.

FIG. 16A illustrates the mean value of resistivity (top) and phase angle (bottom) vs. the excitation frequency for three different tissues: healthy tissue (N), non-transmural and transmural infarcted scar (IS_N and IS_T, respectively). **FIG. 16B** illustrates the mean values of resistivity (top) and phase angle (bottom) at 4 selected frequencies (1, 41, 307 and 1000 kHz) for the three tissues (*** = p<0,001 ; ** = p<0,01).

As shown in **FIG. 16A and 16B**, the mean impedance values during the cardiac cycle of the normal myocardium declines significantly at increasing current frequencies (N: 285.5±10.4 vs. IS_N: 216.4±7.3 vs. IS_T: 155.5±6 Ω·cm, at 41 kHz; p<0.001) and the phase angle shows a negative relaxation that reaches a maximum at about 307 kHz (N: -5.6±0.4 vs. IS_N: -4±0.4 vs. IS_T: -1.7±0.2º, at 41 kHz; p<0.001). In contrast, the infarct scar shows lower resistivity values and less marked phase angle deviation at all frequencies.

Moreover, the curves of frequency dependence of resistivity and phase angle depict a progressive attenuation towards the sites as the recording site moves to areas with transmural necrosis. The current frequencies that better differentiate the transmural and non-transmural scar are 1 kHz, 41 kHz and 307 kHz for resistivity and 41 kHz, 307 kHz and 1 MHz for the phase angle.

FIG. 17 illustrates a linear correlation between myocardial resistivity (upper-left) / phase angle (lower-left) and the percentage of fibrosis. White filled circles correspond to samples with <10% fibrosis, gray triangles to samples with 10% to 70% of fibrosis and black squares to samples with fibrosis higher than 70%. As illustrated in the figure, tissue samples analyzed taken at the sites with corresponding impedance measurements show that myocardial resistivity correlates negatively with the degree of fibrosis ($r=-0.86$ at $f=1kHz$, $p<0.001$) whereas a positive correlation is observed between phase angle and the fibrotic content ($r=0.84$ at $f=41kHz$, $p<0.001$). The best correlation coefficient is obtained at 1 kHz for myocardial resistivity and 41 kHz for phase angle (Table 1).

FIG. 18 illustrates the comparative pattern of the Cole impedance model obtained in normal (N: white), non-transmural scar (IS_N: grey) and infarcted transmural scar (IS_T: black). As the recording site moved from the normal region towards the non-transmural and transmural infarcted area, the Cole arc showed two main changes: a progressive decrease of the area under the curve and a left and down shift towards lower resistivity values (real and imaginary components, respectively). Table 2 summarizes the mean values of the Cole parameters (R_0, R_{inf} ,α and f_c) in 59 tissue samples obtained from the 3 index myocardial regions.

As illustrated in **FIG. 19A**, myocardial tissue electrical resistivity in the normal myocardium depicts a phasic pattern during the cardiac cycle: a peak shortly after the R wave and a minimum value appear in the region of the T wave. As illustrated in **FIG. 19B**, the non-transmural infarcted region depicts a pattern similar to normal myocardium. By contrast, as illustrated in **FIG. 19C** the transmural necrotic region

shows a marked attenuation of the magnitude of the resistivity changes with a delayed occurrence of the maximal and minimal resistivity values.

Univariate analysis showed that the impedance parameters that detect differences between the three tissue categories are the mean value of the resistivity and the phase angle during the cardiac cycle at 41 kHz. Using multinomial logistic regression it has been found that the resistivity has the highest probability to correctly classify between healthy tissue, non-transmural and transmural infarct scar.

To further assess the predictive ability of different impedance parameters to discriminate between scar tissues with transmural and non-transmural affectation, the analysis of ROC (receiver operating characteristic) curves were used. Table 3 shows the accuracy of the ROC curve assessed by the area under the ROC curve (AUC) for all the different studied variables with its statistical significance levels. Resistivity, phase angle, resistivity amplitude, delay t_1, R_0, R_{inf}, and f_c exhibit good values of AUC with significant p-values, being f_c the best parameter. As illustrated in **FIG. 20** which is a multiparametric analysis showing that a combination of resistivity and f_c improve the predictive ability to discriminate between both fibrotic tissues.

Although only a number of examples have been disclosed herein, other alternatives, modifications, uses and/or equivalents thereof are possible. Furthermore, all possible combinations of the described examples are also covered. Thus, the scope of the present disclosure should not be limited by particular examples, but should be determined only by a fair reading of the claims that follow.

Further, although the examples described with reference to the drawings comprise computing apparatus/systems and processes performed in computing apparatus/systems, the invention also extends to computer programs, particularly computer programs on or in a carrier, adapted for putting the system into practice.

CLAIMS

1. A method of assessing a cardiac tissue, comprising:

selecting an area of interest of the cardiac tissue;

identifying one or more measurement locations in the selected area of interest;

placing an electrocatheter probe at the one or more measurement locations;

providing a broadband spectrum signal to the one or more measurement locations using the electrocatheter probe;

identifying a diastolic phase of the cardiac cycle;

measuring impedance of the cardiac tissue during the identified diastolic phase;

identifying a systolic phase of the cardiac cycle;

measuring impedance of the cardiac tissue during the identified systolic phase;

assessing said cardiac tissue based on said diastolic and systolic impedance measurements.

2. Method according to claim 1, wherein placing an electrode probe on the one or more measurement locations comprises

selecting a temporal sequence of measurements on a plurality of measurement locations;

placing the impedance measurement probe successively at each of the plurality of measurement locations.

3. Method according to claim 1 or 2, wherein the identified systolic phase comprises a pre-ejection phase and an ejection phase and measuring impedance during the systolic phase comprises

measuring impedance during the pre-ejection phase; and

measuring impedance during the ejection phase.

4. Method according to claim 1 or 2, wherein the impedance measurements are obtained between two electrocatheters, one configured to be placed at a location of the cardiac tissue and the other at another location of the cardiac tissue or of the body.

5. Method according to claim 1 or 2, wherein the impedance measurements are obtained between an electrocatheter configured to be placed at a location of the cardiac tissue and a selected electrode placed at another body location.

6. Method according to any of claims 1 to 5 further comprising,

classifying the measurement location as either a normal region or an infarct scar region in response to said impedance measurement.

7. Method according to claim 6, further comprising identifying resistivity and phase angle parameters of the impedance measurements and wherein classifying comprises correlating the identified resistivity and/or the phase angle components with a fibrosis percentage.

8. Method according to claim 7, wherein the broadband signal comprises multiple current frequencies between 1kHz and 1MHz.

9. Method according to claim 7, wherein the broadband current signal comprises one or more frequencies selected from a 1kHz, 41kHz, 307 kHz and 1 MHz frequencies.

10. Method according to any of claims 7 to 9, further comprising identifying a transmurality percentage of the cardiac tissue.

11. Method according to any of claims 1 to 10, wherein the impedance measurements are in vivo measurements.

12. Method according to claim 11, further comprising ablating the ischemic zone.

13. Method according to any of claims 1 to 12, further comprising recording of a number of spectra along the cardiac cycle that allow reconstructing time-domain signals at different and simultaneous frequencies and use indicators of the signals shape to assess the cardiac tissue.

14. Method according to claim 13, wherein the indicators of the signals shape comprise one or more of (i) a slope of the signals in selected points, (ii) number and type of local maxima and minima of the signals, and (iii) a spectral content.

15. Method according to any of claims 1 to 14, wherein the systolic and diastolic phases are identified by synchronism with other physiological signals comprising one or more of (i) an ECG signal, (ii) a pressure signal and (iii) a flux signal, (iv) a maximum and minimum of impedance or admittance related signals.

16. Method according to any of claims 1 to 15, wherein measuring impedance comprises measuring one or more of the intrinsic variables of impedance or measuring admittance and calculating impedance thereafter as a function of such measurements.

17. Method according to claim 16, wherein measuring impedance further comprises taking into account the values and the absolute or relative changes of the magnitude or phase angle or their alternative representations as real and imaginary part, and/or the model parameters after fitting any of the aforementioned variables spectrum to a mathematical model, their time course or their values in selected points of the cardiac cycle.

18. Method according to any of claims 15 to 17, wherein the assessing the tissue comprises deriving the state of the tissue from pathology-dependent delays between the reference signals (arterial or left ventricular pressure, ECG) and the impedance related signals.

19. Method according to any of claims 15 to 17, wherein the tissue-state estimators are derived from pathology-dependent shape and/or area of the figure resulting of the representation of an impedance-related variable at one or several frequencies and the ventricle pressure.

20. A device, comprising:

means for selecting an area of interest of a cardiac tissue;

means for identifying one or more measurement locations in the selected area of interest;

means for placing an electrocatheter probe at the one or more measurement locations;

means for providing a broadband signal to the one or more measurement locations using the electrocatheter probe;

means for identifying a diastolic phase of the cardiac cycle;

means for measuring impedance of the cardiac tissue during the identified diastolic phase;

means for identifying a systolic phase of the cardiac cycle;

means for measuring impedance of the cardiac tissue during the identified systolic phase;

means for assessing said cardiac tissue based on said diastolic and systolic impedance measurements.

21. Device according to claim 20, wherein the means for placing an electrode probe on the one or more measurement locations comprises

means for selecting a temporal sequence of measurements on a plurality of measurement locations;

means for placing the impedance measurement probe successively at each of the plurality of measurement locations.

22. Device according to claim 20 or 21, wherein the identified systolic phase comprises a pre-ejection phase and an ejection phase and the means for measuring impedance during the systolic phase comprises

means for measuring impedance during the pre-ejection phase; and

means for measuring impedance during the ejection phase.

23. Device according to claim 22, wherein the means for measuring impedance comprise two electrocatheters, one configured to be placed at a location of the cardiac tissue and the other at another location of the cardiac tissue or of the body.

24. Device according to claim 23, wherein the means for measuring impedance comprise an electrocatheter configured to be placed at a location of the cardiac tissue and a selected electrode placed at another body location.

25. Device according to any of claims 20 to 24 further comprising,

means for classifying the measurement location as either a normal region or an infarct scar region in response to said impedance measurement.

26. Device according to claim 25, further comprising means for identifying resistivity and phase angle parameters of the impedance measurements and wherein the means for classifying comprises means for correlating the identified resistivity and/or the phase angle components with a fibrosis percentage.

27. Device according to claim 26, wherein the broadband signal comprises multiple current pulses with frequencies between 1kHz and 1MHz.

28. Device according to claim 27, wherein the broadband signal comprises one or more current pulses having a frequency selected from a 1kHz, 41kHz, 307 kHz and 1 MHz frequencies.

29. Device according to any of claims 25 to 27, further comprising means for identifying a transmurality percentage of the cardiac tissue.

30. Device according to claim 29, further comprising means for identifying an infarct scar tissue zone as an ischemic zone.

31. Device according to claim 30, wherein the means for measuring impedance are means for in vivo measuring impedance.

32. Device according to claim 31, further comprising means for ablating the ischemic zone.

33. Device according to any of claims 20 to 32, further comprising means for recording of a number of spectra along the cardiac cycle that allow reconstructing time-domain signals at different and simultaneous frequencies and use indicators of the signals shape to assess the cardiac tissue.

34. Device according to claim 33, wherein the indicators of the signals shape comprise one or more of (i) a slope of the signals in selected points, (ii) number and type of local maxima and minima of the signals, and (iii) a spectral content.

35. Device according to any of claims 31 to 34, wherein means for identifying the systolic and diastolic phases use synchronism with other physiological signals comprising one or more of (i) an ECG signal, (ii) a pressure signal and (iii) a flux signal, (iv) a maximum and minimum of impedance or admittance related signals, to identify said phases.

36. Device according to any of claims 31 to 35, wherein the means for measuring impedance comprises means for measuring one or more of the intrinsic variables of impedance or means for measuring admittance and calculating impedance thereafter as a function of such measurements.

37. Device according to claim 36, wherein the means for measuring impedance take into account the values and the absolute or relative changes of the magnitude or phase angle or their alternative representations as real and imaginary part, and/or the model parameters after fitting any of the aforementioned variables spectrum to a mathematical model, their time course or their values in selected points of the cardiac cycle.

38. Device according to any of claims 35 to 37, wherein the means for assessing the cardiac tissue are configured to derive assessment from pathology-dependent delays between the reference signals (arterial or left ventricular pressure, ECG) and the impedance related signals.

39. Device according to any of claims 35 to 37, wherein the means for assessing the cardiac tissue are configured to derive assessment from pathology-dependent shape and/or area of the figure resulting of the representation of an impedance-related variable at one or several frequencies and the ventricle pressure.

40. A device, comprising:

an arbitrary waveform generator (AWG) to deliver one or more broadband frequency current signals having an amplitude and a duration lasting over a time period associated with one or more cardiac cycles;

a multielectrode probe, coupled to the AWG, configured to apply the broadband frequency current signal in vivo to a cardiac tissue and measure impedance of the cardiac tissue;

an acquisition module (AM) comprising:

an electrocardiograph (ECG) recorder;

a blood pressure recorder;

a controller, coupled to the AWG and to the AM and configured to

receive the impedance measurements during the duration of the broadband signal;

receive the recording of the acquisition module during the duration of the broadband signal;

identify a systolic or diastolic phase of a cardiac cycle;

correlate the impedance measurements with the identified phase of the cardiac cycle;

identify the cardiac tissue as transmural or non-transmural in response to said correlation.

41. The device according to claim 40, wherein the multielectrode probe comprises a transcatheter probe.

42. The device according to claim 41, wherein the transcatheter probe comprises

a tip electrode arranged at or near a tip of the transcatheter probe; and

one or more ring electrodes arranged around the transcatheter probe and at one or more distances from the tip electrode, respectively.

43. The device according to claim 41 or 42, wherein the transcatheter probe comprises an array of four electrodes arranged at a side or at a tip of the transcatheter probe

44. A device according to any of claims 41 to 43, wherein the transcatheter probe comprises two electrocatheters configured to be placed at different locations of the cardiac tissue.

45. The device according to any of claims 41 to 44, wherein the transcatheter probe comprises

an ablation electrode at a tip of the transcatheter probe.

46. The device according to claim 45, further comprising a mapping tool to identify an ablation zone comprising all identified transmural and non-transmural ischemic tissue in a region of interest.

47. The device according to claim 46, wherein the multielectrode probe is further configured to apply an ablation current to the ablation electrode to ablate the identified ablation zone.

48. The device according to any of claims 40 to 47, wherein the controller comprises a front-end to select and adapt the signals to and from the electrodes and a processor to synchronize the generation and the acquisition, control the acquisition sequence and send the results to an external processing and visualization system, the external processing and visualization system being suitable for acquiring time-frequency information of quasi-static electrical impedance spectra in a given location of the myocardium and in several temporal points of the cardiac cycle.

49. The device according to claim 48, wherein the front-end is configured to be adaptable to several electrode configurations of 2, 3 or 4 electrode configurations and switch between them.

50. A system comprising:

a device according to any of claims 40 to 49,

an external processing apparatus, connectable to the device via a communication link, the external processor apparatus configured to run an application to determine the suitable waveform to be uploaded in the AWG, the acquisition strategy, and to apply the algorithms to obtain the values of the tissue state estimators from the time-frequency characteristics of the measured impedance signals.

51. A controller, comprising:

a signal selector module, configured to be coupled to an arbitrary waveform generator (AWG), to provide to the AWG parameters of a broadband current pulse signal to be applied on a cardiac tissue;

a receiver configured to be coupled to an acquisition module to receive impedance measurements and ECG and blood pressure recordings from the acquisition module;

a processing module, configured to identify a systolic and/or diastolic phase of the cardiac cycle as a function of said received recordings;

an assessment module, configured to identify a state of the cardiac tissue as a function of the impedance measurements and the identified phase.

52. The controller according to claim 51, wherein the controller is configured to identify a state of the cardiac tissue as a fibrosis state.

53. The controller according to claim 52, wherein the controller is configured to generate a transmurality fibrosis map of the cardiac tissue as a function to the impedance measurements and the identified phase.

54. The controller according to claim 53, further configured to be coupled to an ablation tool to provide an ablation map based on the transmurality fibrosis map in conjunction to the voltage map.

55. A computer program product comprising program instructions for causing a computing system to perform a method according to any of claims 1 to 19.

56. A computer program product according to claim 55, embodied on a storage medium.

57. A computer program product according to claim 55, carried on a carrier signal.

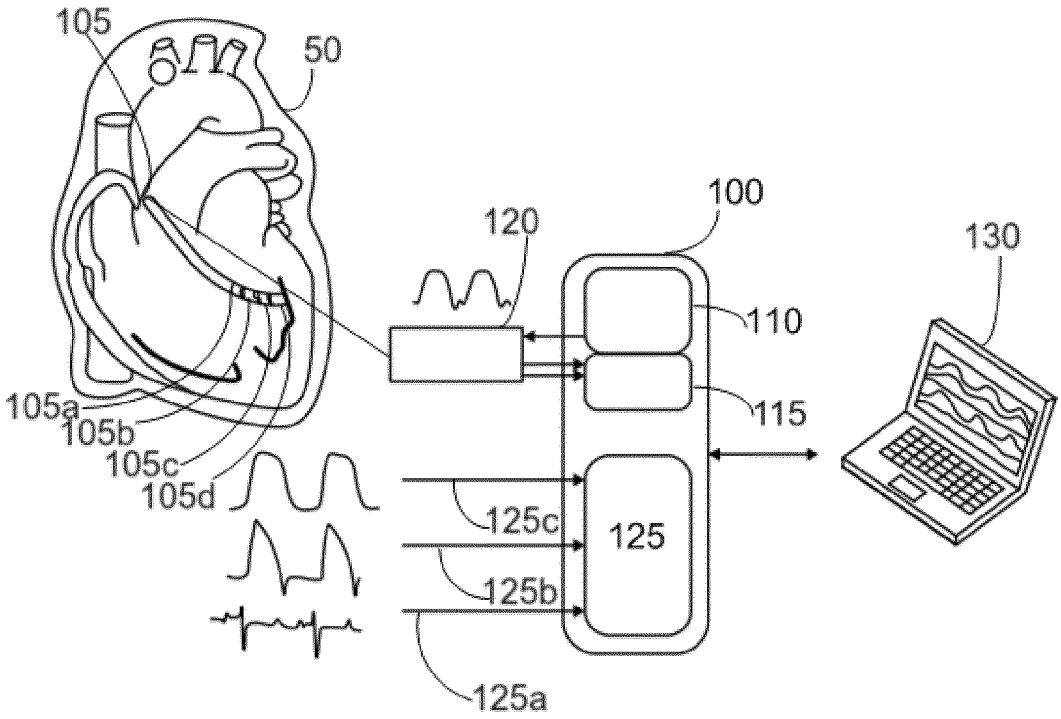
105
50
100
120
130
110
115
105a
105b
105c
105d
125c
125
125b
125a

Fig. 1A

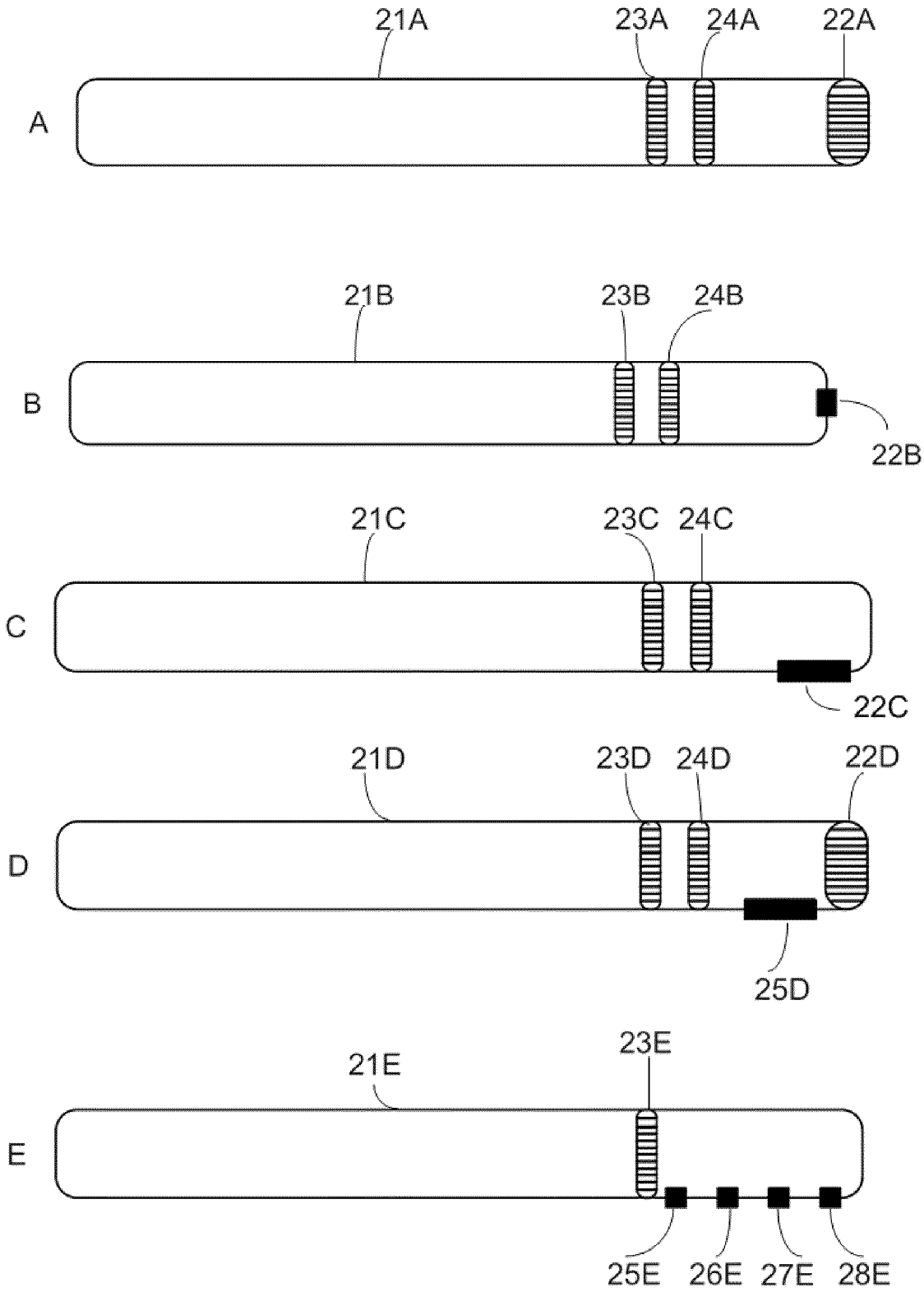
21A
23A
24A
22A
A
21B
23B
24B
B
22B
21C
23C
24C
C
22C
21D
23D
24D
22D
D
25D
23E
21E
E
25E
26E
27E
28E

Fig. 1B

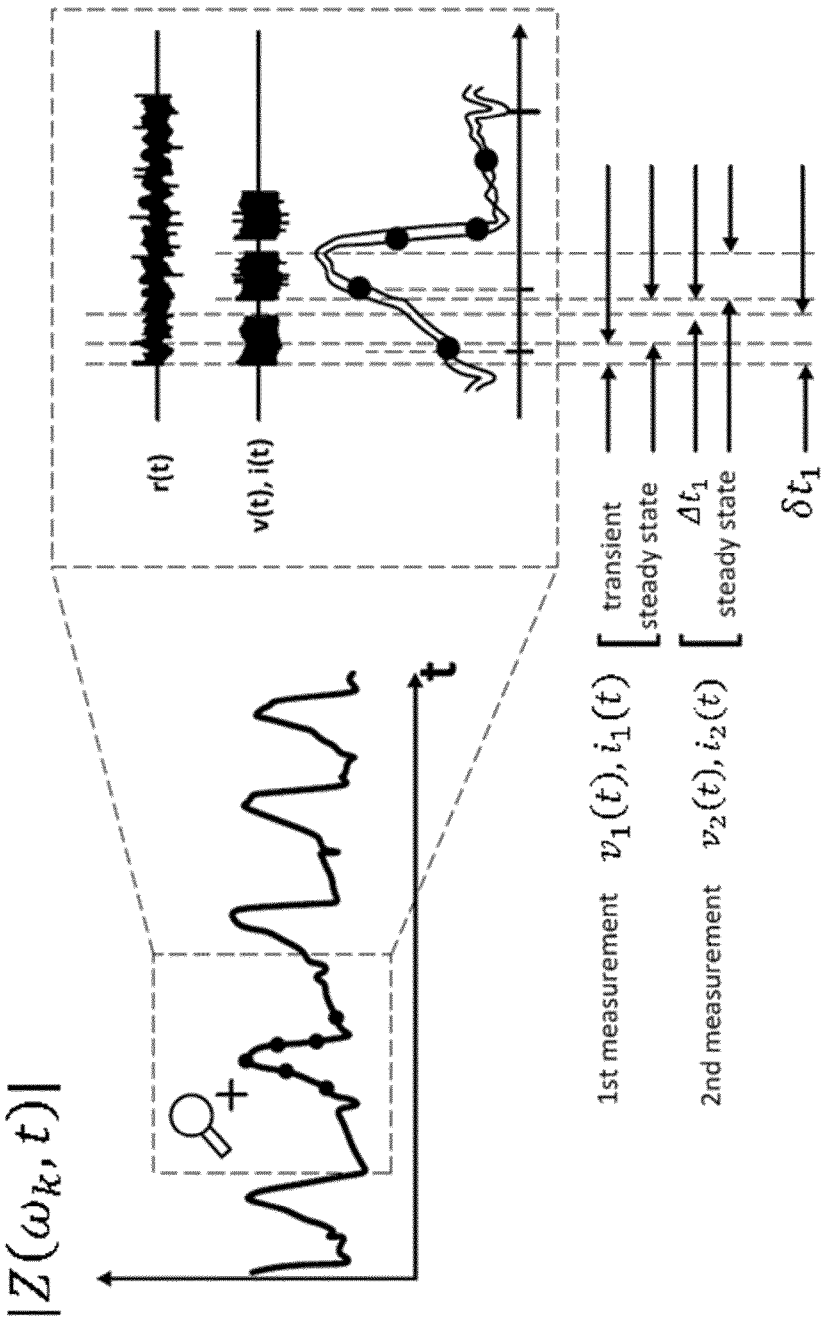
$|Z(\omega_k, t)|$
t
r(t)
v(t), i(t)
1st measurement
$v_1(t), i_1(t)$
transient
steady state
Δt_1
2nd measurement
$v_2(t), i_2(t)$
steady state
δt_1

Fig. 2

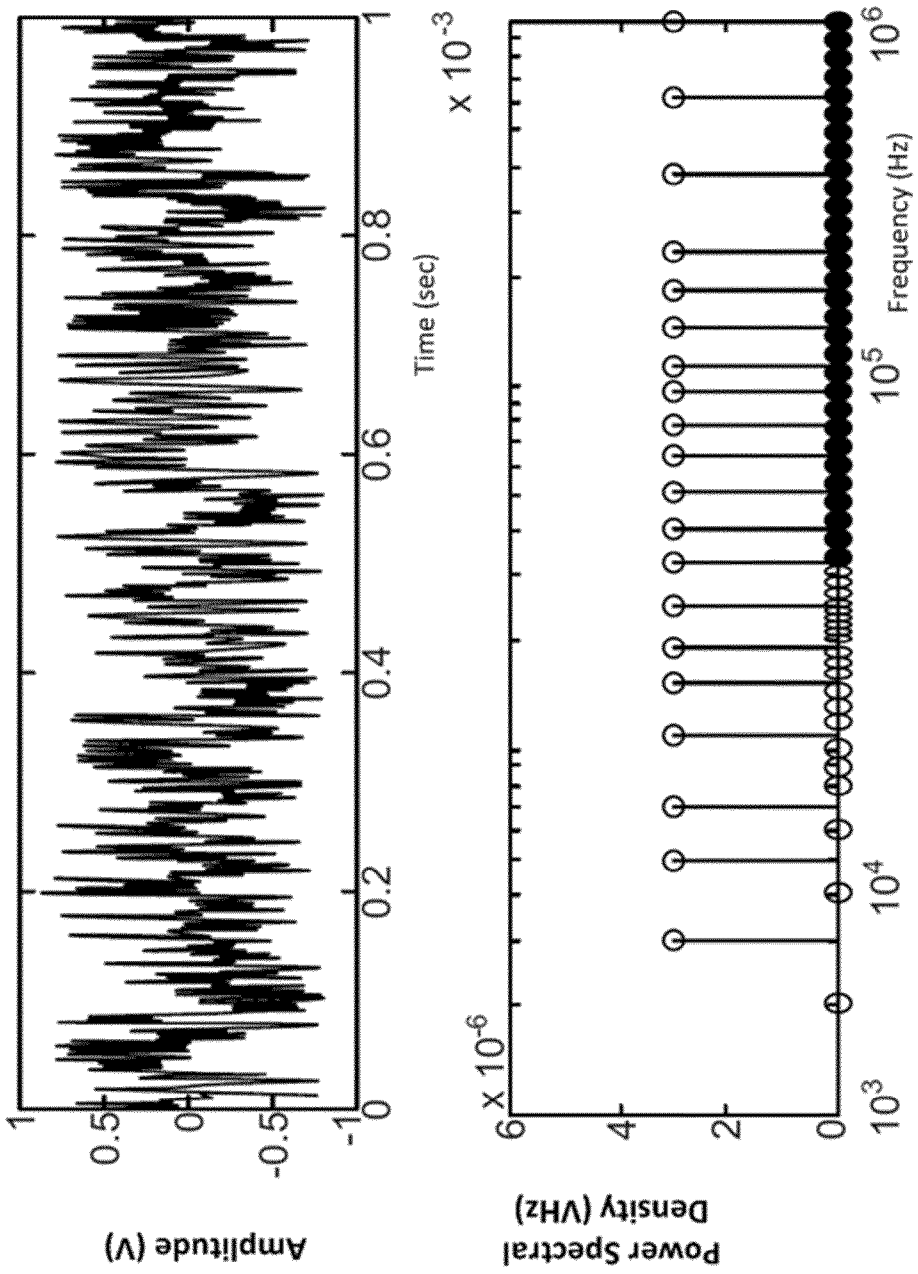
Amplitude (V)
1
0.5
0
-0.5
-1
0
0.2
0.4
0.6
0.8
1
Time (sec)
x 10^-3
Power Spectral Density (V/Hz)
x 10^-6
6
4
2
0
10^3
10^4
10^5
10^6
Frequency (Hz)

Fig. 3

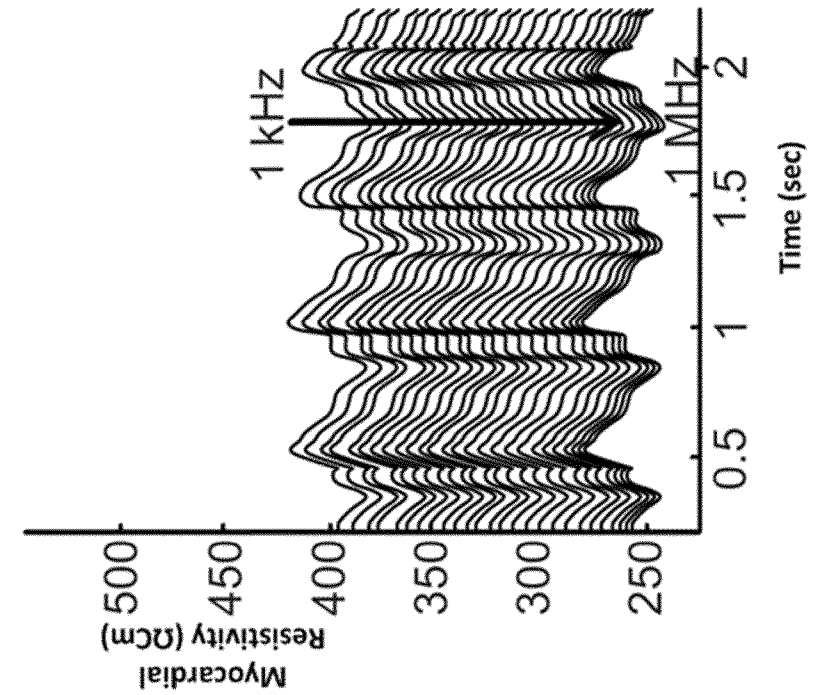
1 kHz
1 MHz
Time (sec)
0.5
1
1.5
2
Myocardial Resistivity (ΩCm)
250
300
350
400
450
500

Fig. 4B

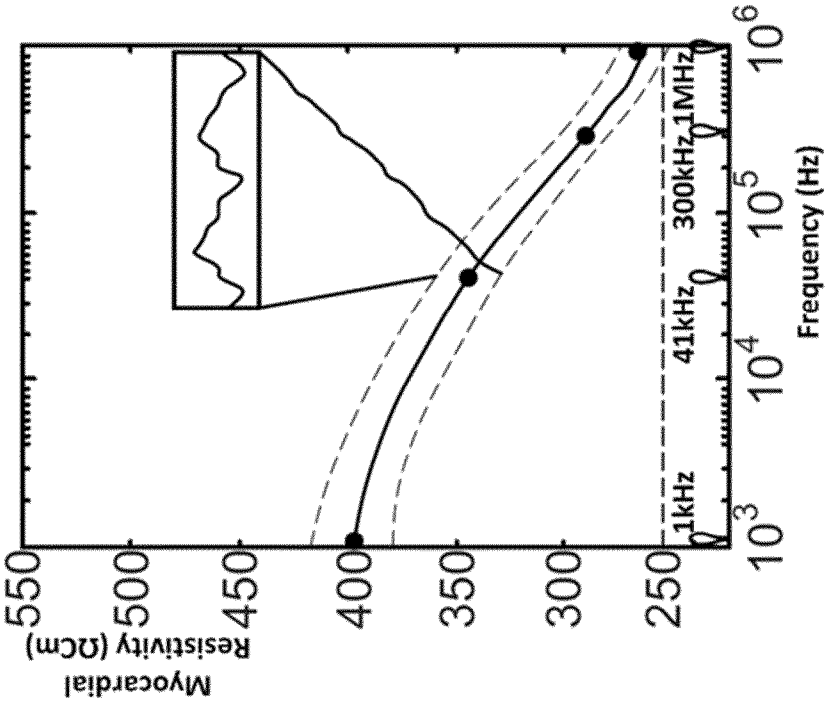
Myocardial Resistivity (ΩCm)
250
300
350
400
450
500
550
Frequency (Hz)
10^3
10^4
10^5
10^6
1kHz
41kHz
300kHz
1MHz

Fig. 4A

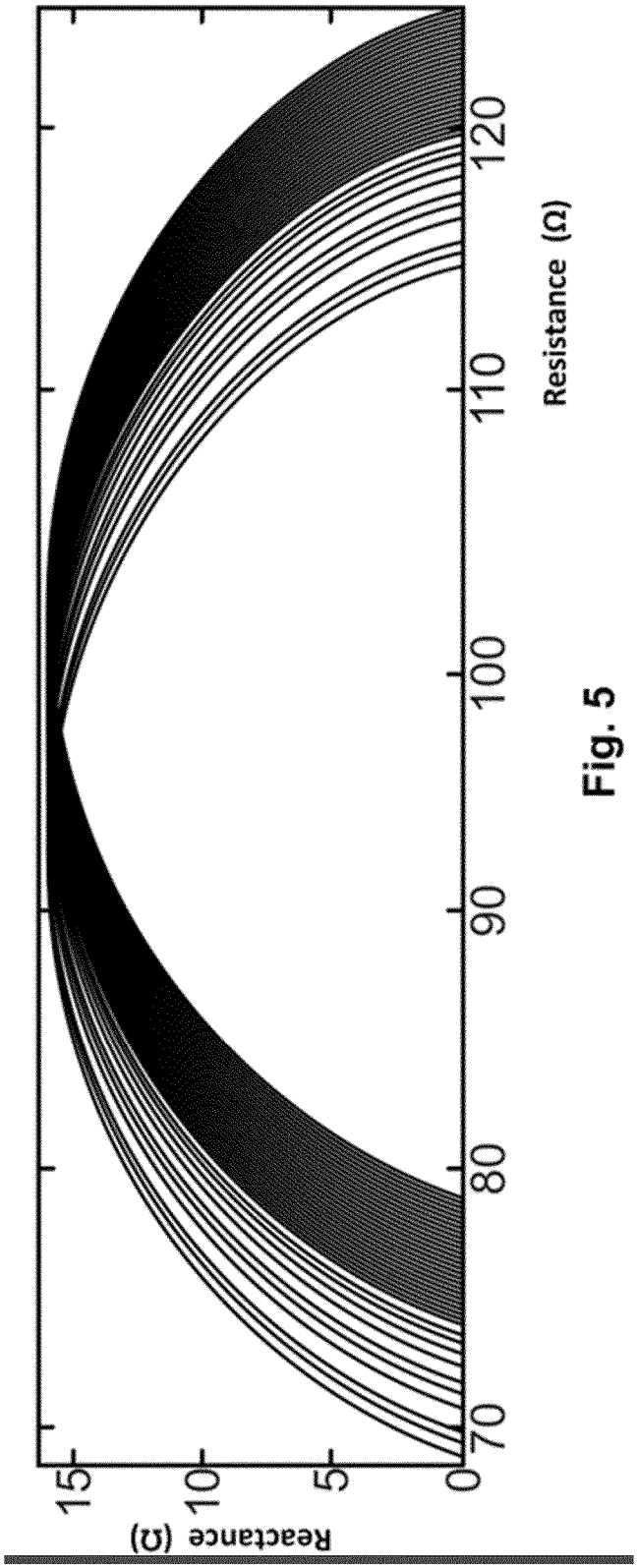

Fig. 5

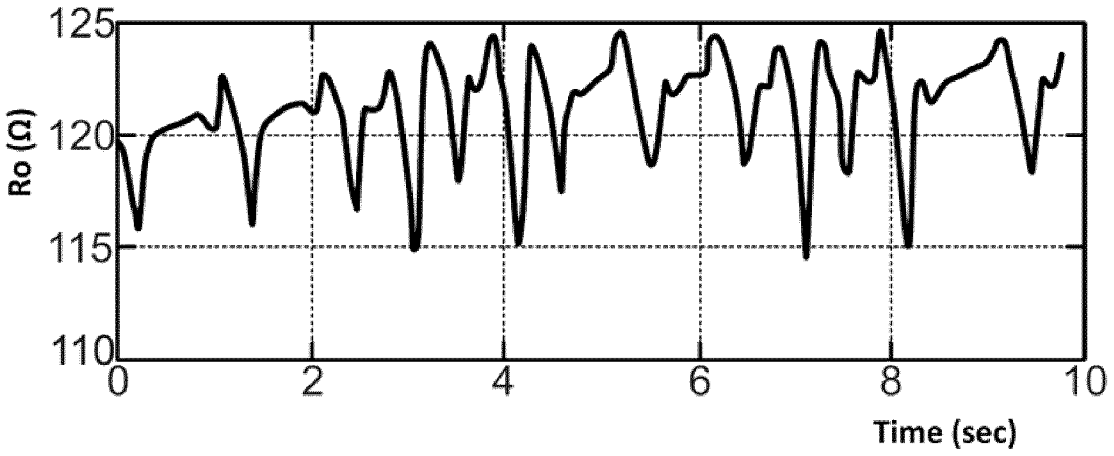
125
120
115
110
Ro (Ω)
0
2
4
6
8
10
Time (sec)

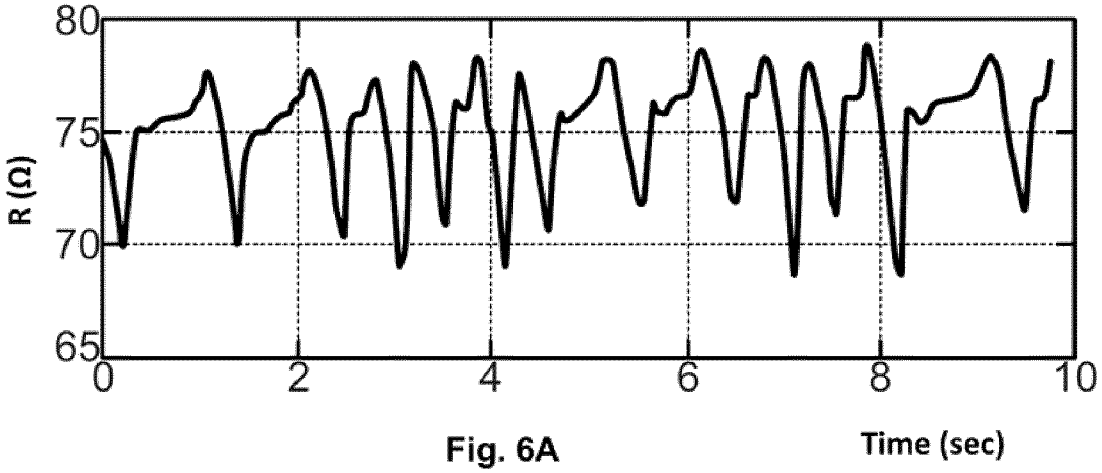
80
75
70
65
R (Ω)
0
2
4
6
8
10
Time (sec)

Fig. 6A

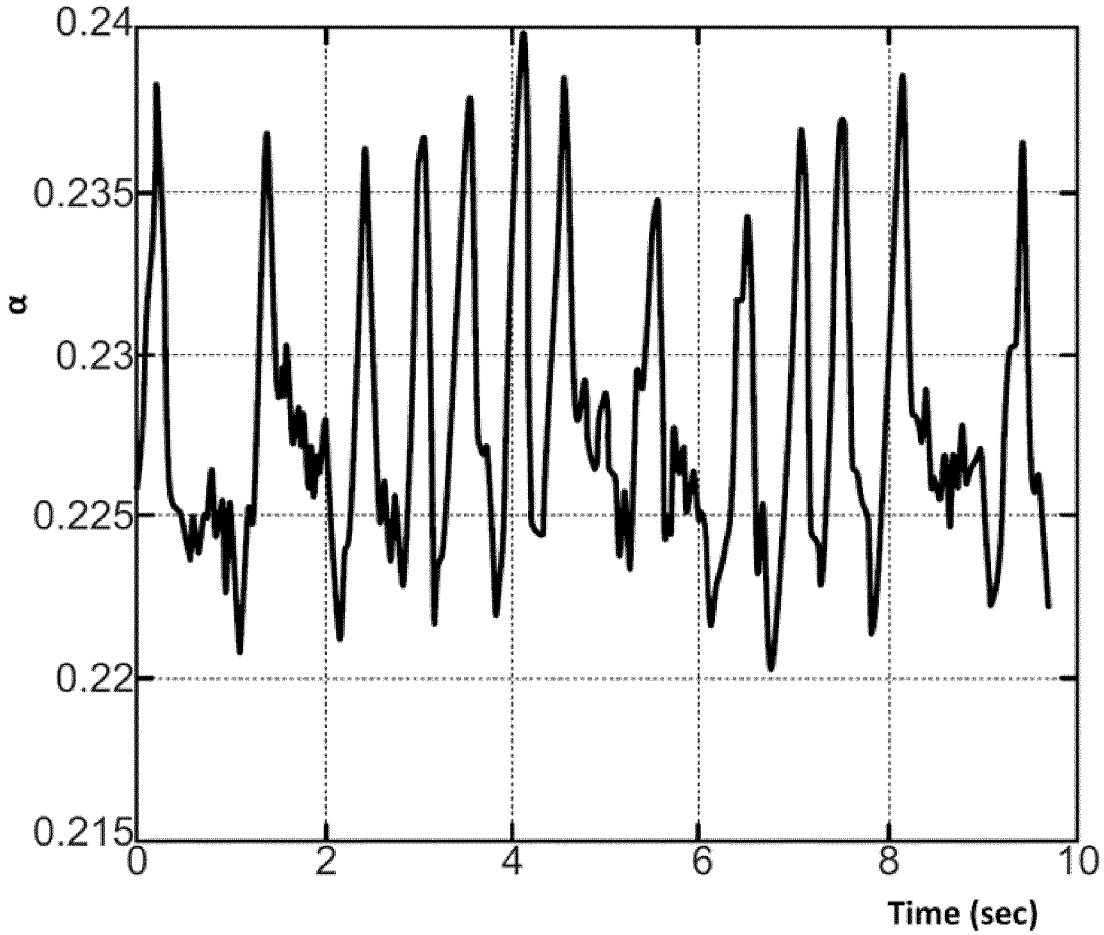

Fig. 6B

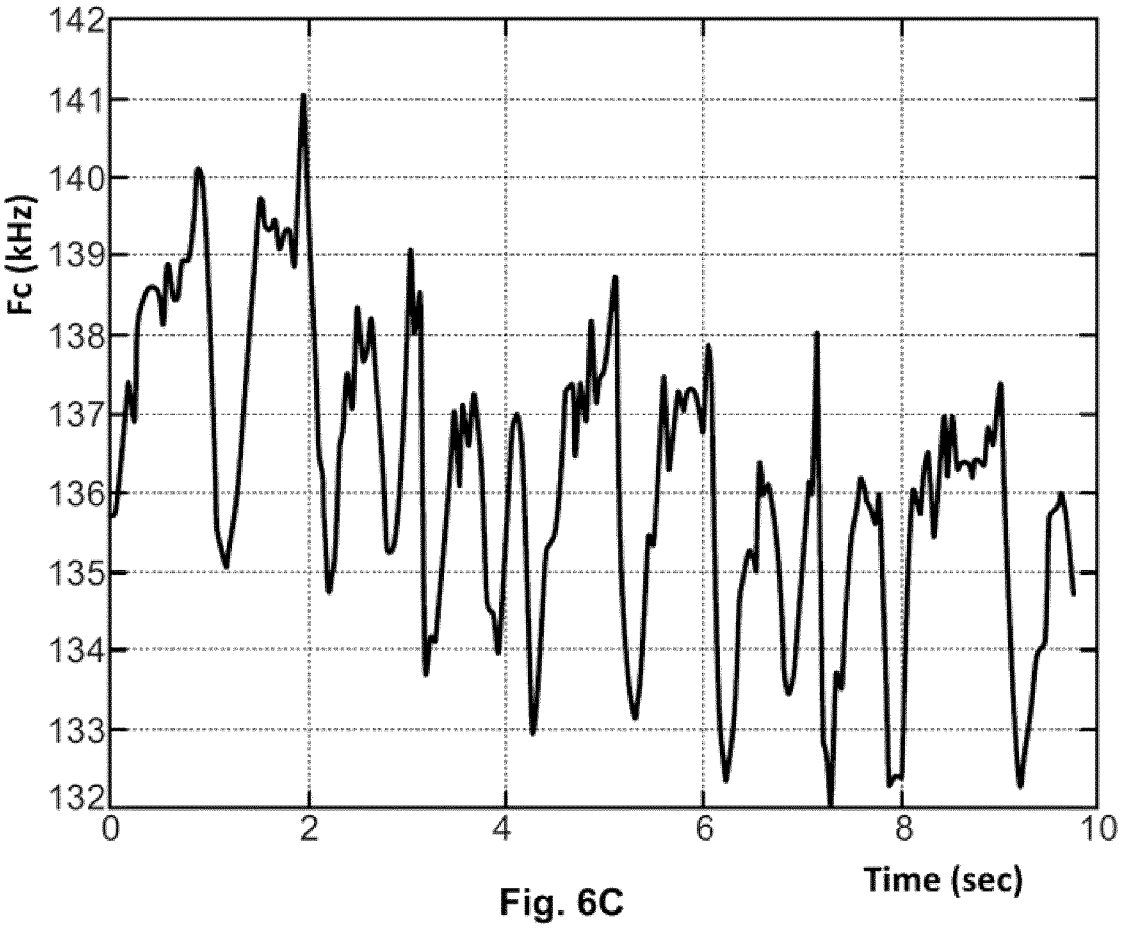
142
141
140
139
138
137
136
135
134
133
132
Fc (kHz)
0
2
4
6
8
10
Time (sec)

Fig. 6C

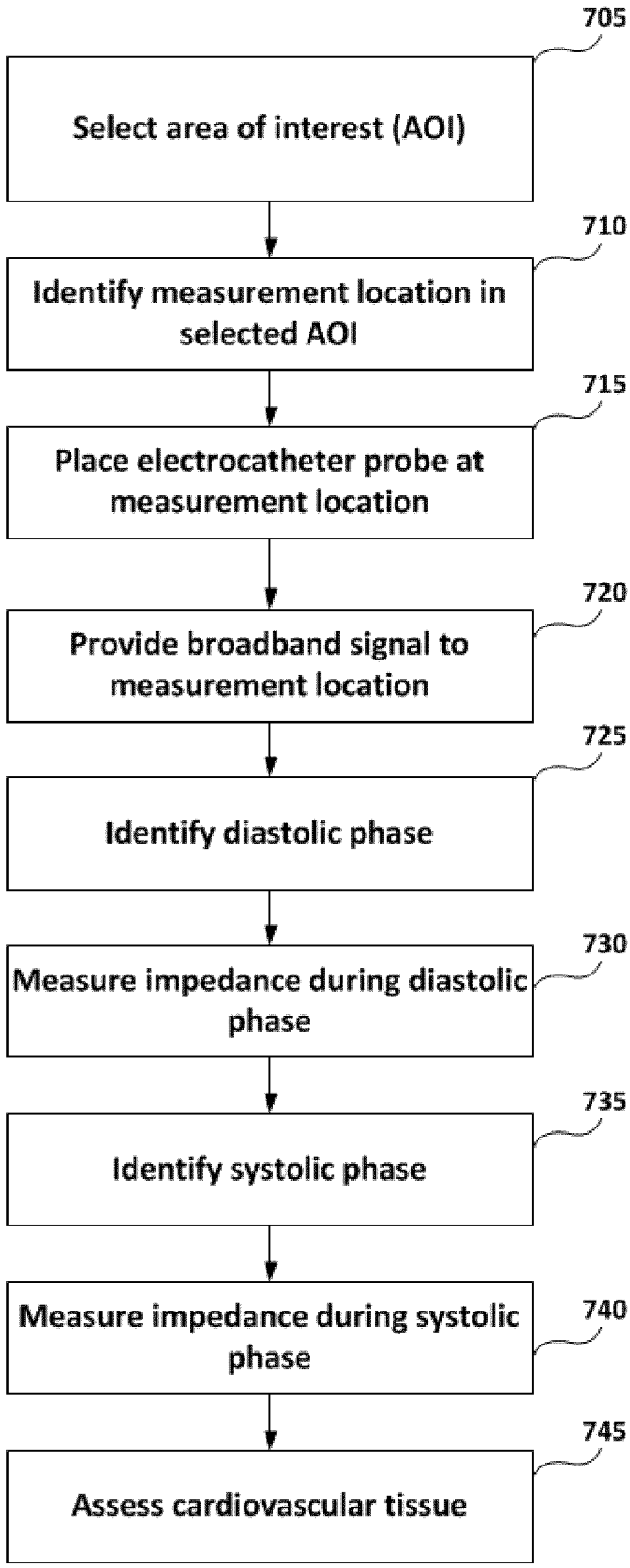
705
Select area of interest (AOI)
710
Identify measurement location in selected AOI
715
Place electrocatheter probe at measurement location
720
Provide broadband signal to measurement location
725
Identify diastolic phase
730
Measure impedance during diastolic phase
735
Identify systolic phase
740
Measure impedance during systolic phase
745
Assess cardiovascular tissue

Fig. 7

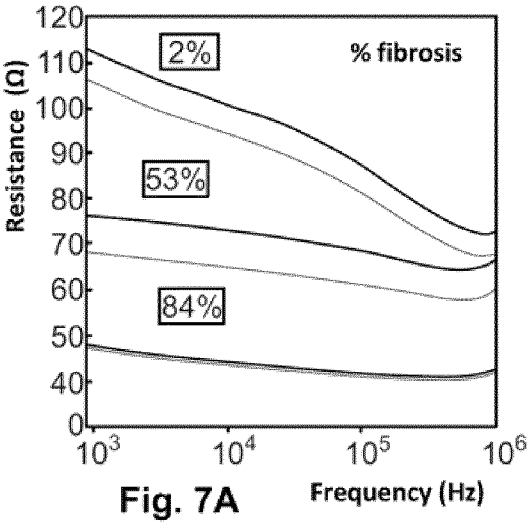

Fig. 7A

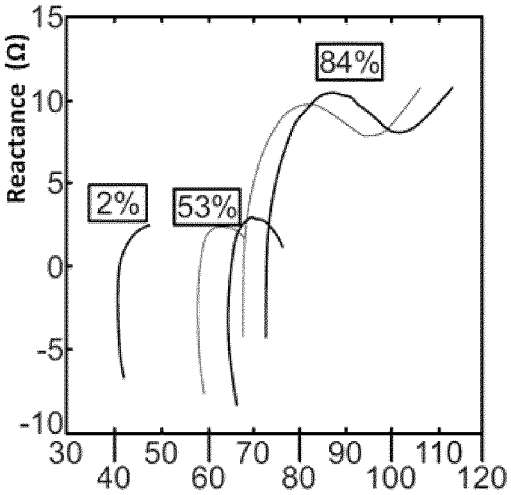

Fig. 7B

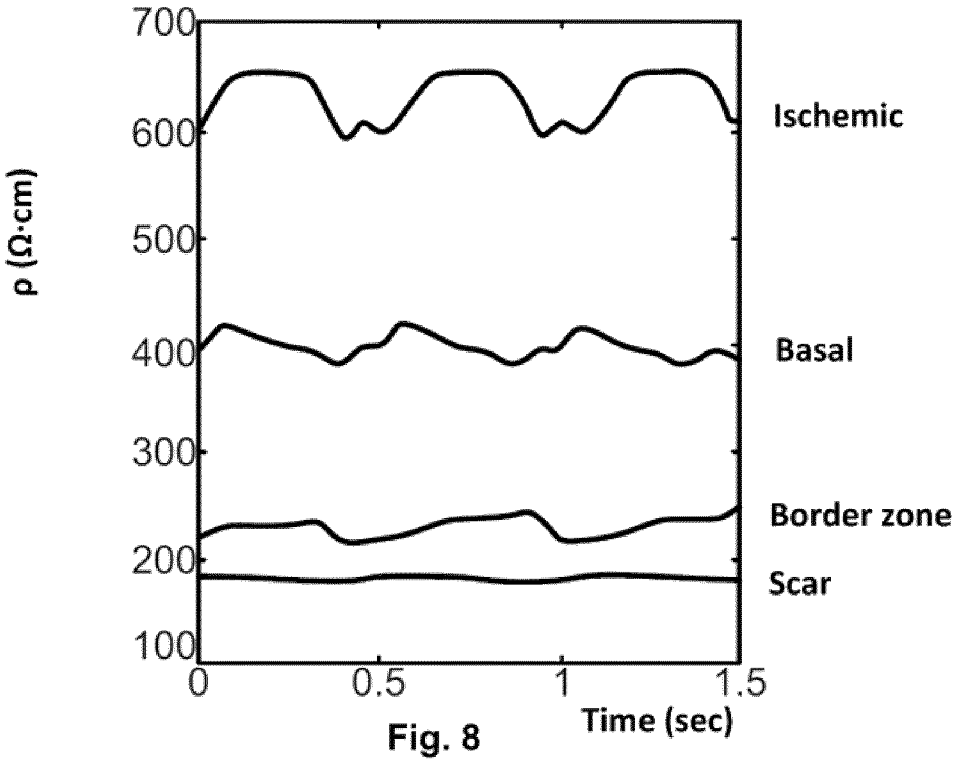

Fig. 8

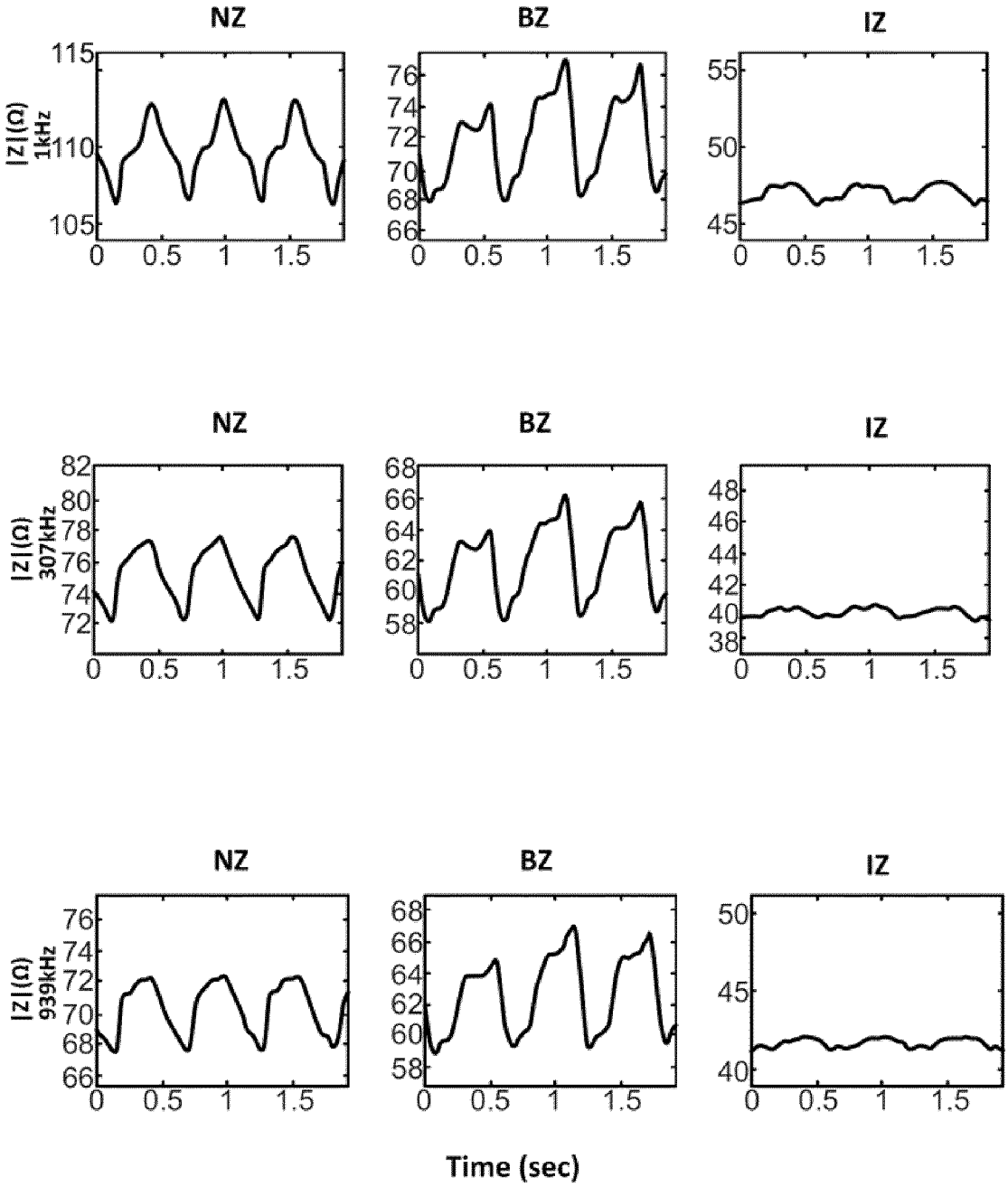
NZ
BZ
IZ
|Z|(Ω) 1kHz
115
110
105
76
74
72
70
68
66
55
50
45
0 0.5 1 1.5
NZ
BZ
IZ
|Z|(Ω) 307kHz
82
80
78
76
74
72
68
66
64
62
60
58
48
46
44
42
40
38
0 0.5 1 1.5
NZ
BZ
IZ
|Z|(Ω) 939kHz
76
74
72
70
68
66
68
66
64
62
60
58
50
45
40
0 0.5 1 1.5
Time (sec)

Fig. 9

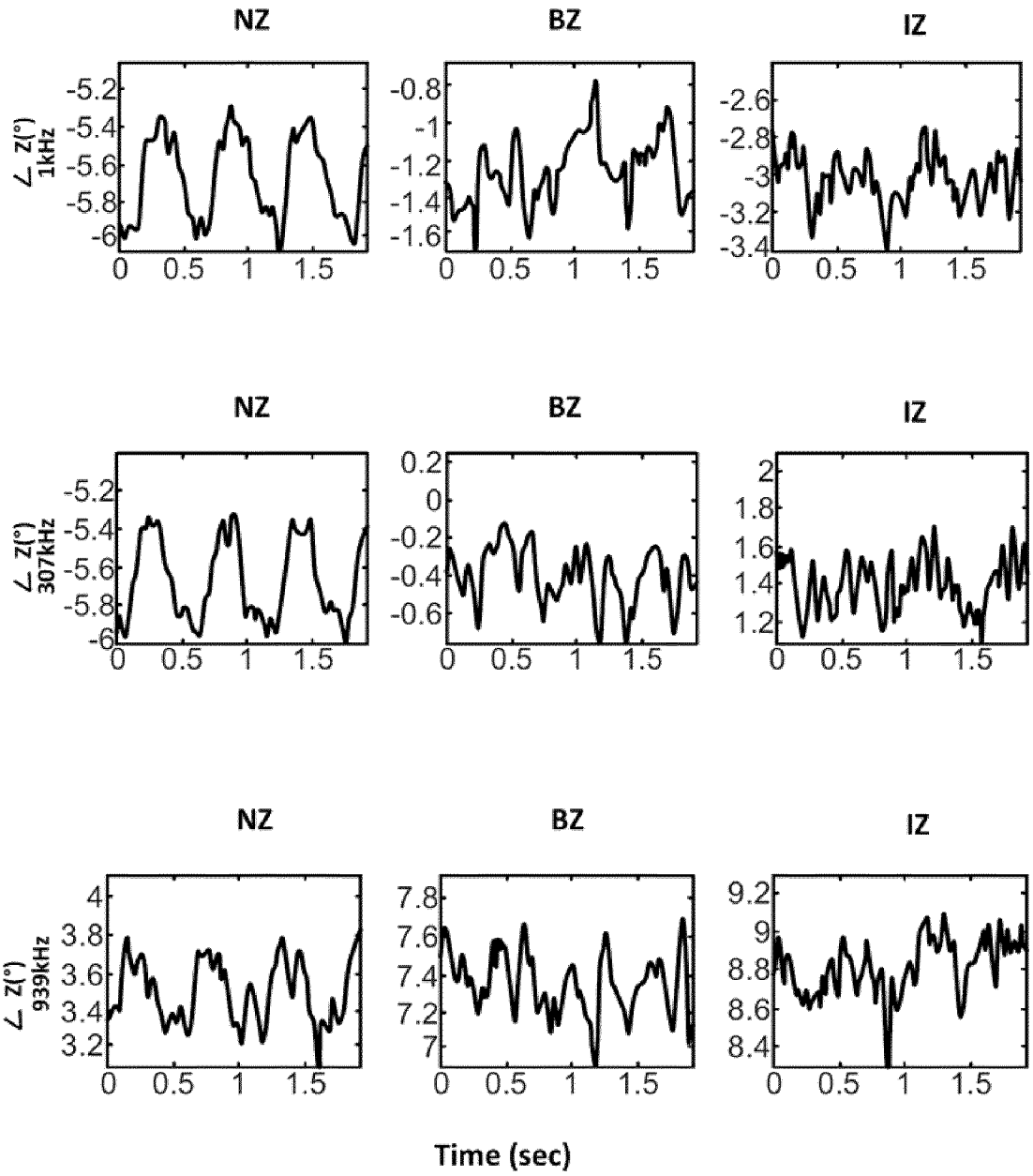
NZ
BZ
IZ
∠ Z(°) 1kHz
-5.2
-5.4
-5.6
-5.8
-6
-0.8
-1
-1.2
-1.4
-1.6
-2.6
-2.8
-3
-3.2
-3.4
NZ
BZ
IZ
∠ Z(°) 307kHz
-5.2
-5.4
-5.6
-5.8
-6
0.2
0
-0.2
-0.4
-0.6
2
1.8
1.6
1.4
1.2
NZ
BZ
IZ
∠ Z(°) 939kHz
4
3.8
3.6
3.4
3.2
7.8
7.6
7.4
7.2
7
9.2
9
8.8
8.6
8.4
0 0.5 1 1.5
Time (sec)

Fig. 10

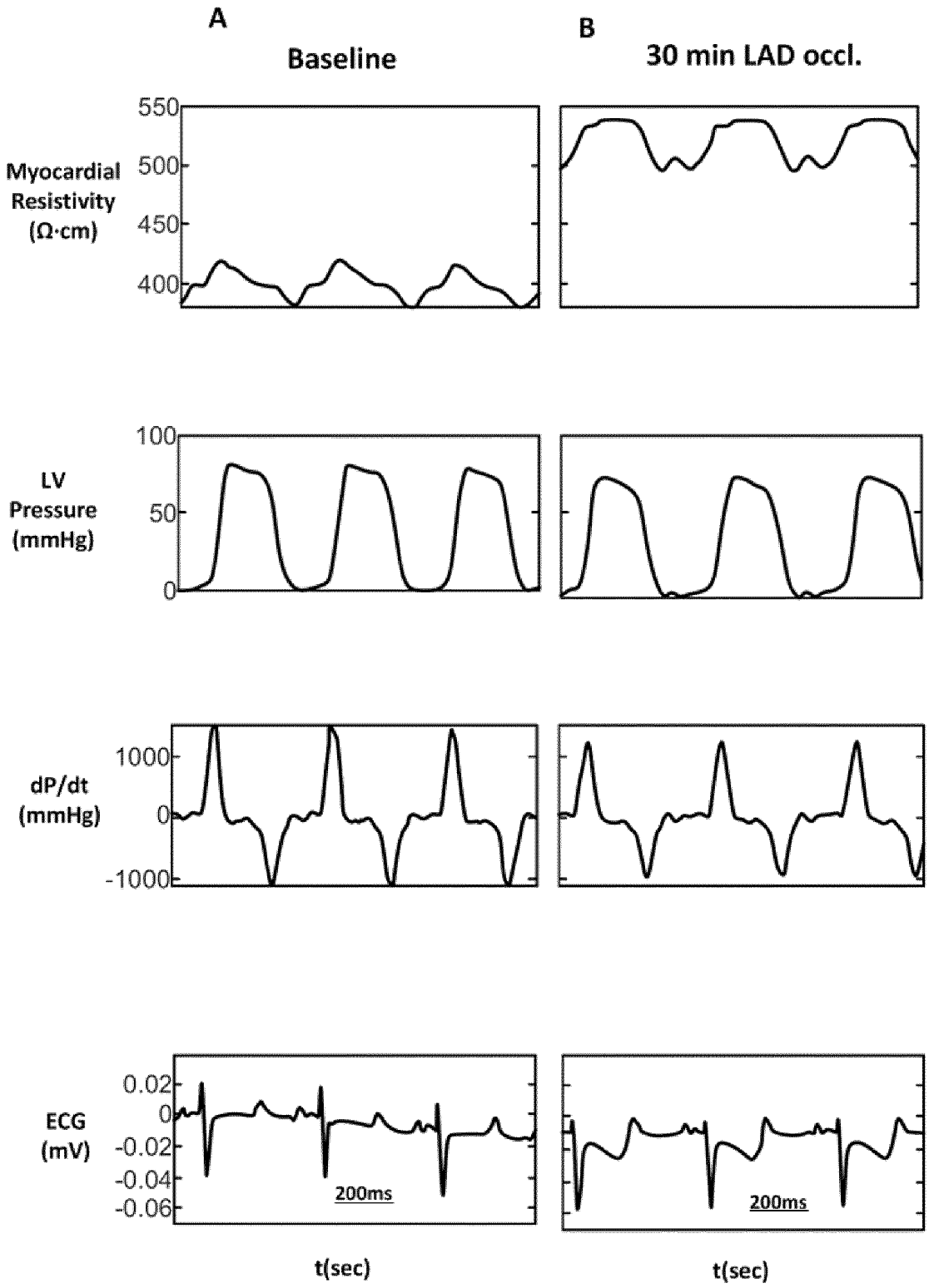
A
Baseline
B
30 min LAD occl.
Myocardial Resistivity (Ω·cm)
550
500
450
400
LV Pressure (mmHg)
100
50
0
dP/dt (mmHg)
1000
0
-1000
ECG (mV)
0.02
0
-0.02
-0.04
-0.06
200ms
200ms
t(sec)
t(sec)

Fig. 11

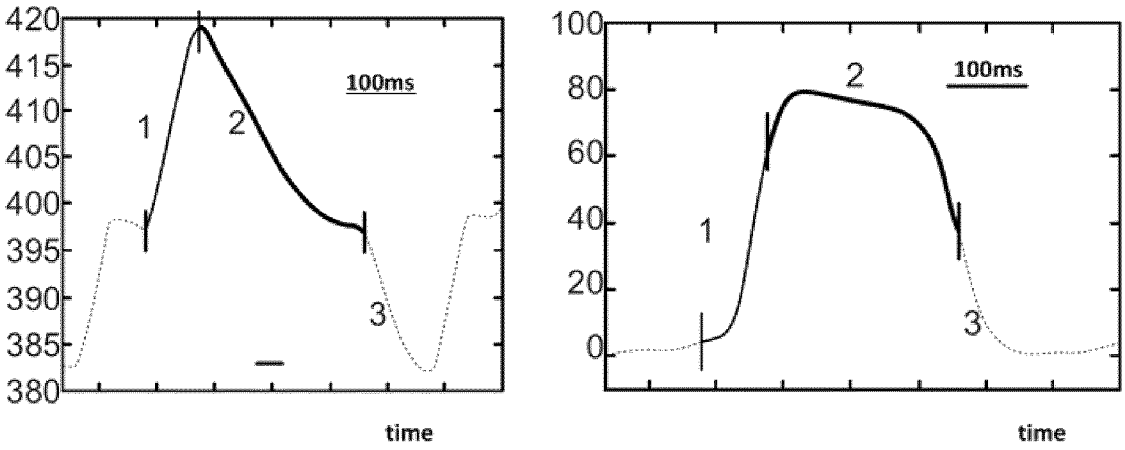

Fig. 12A

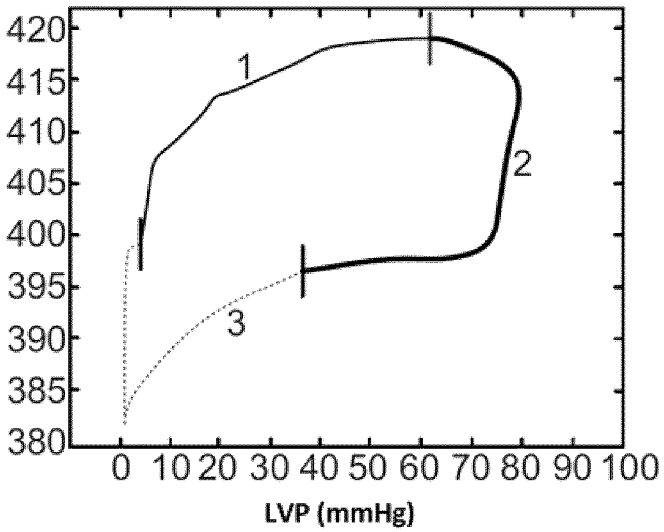

Fig. 12B

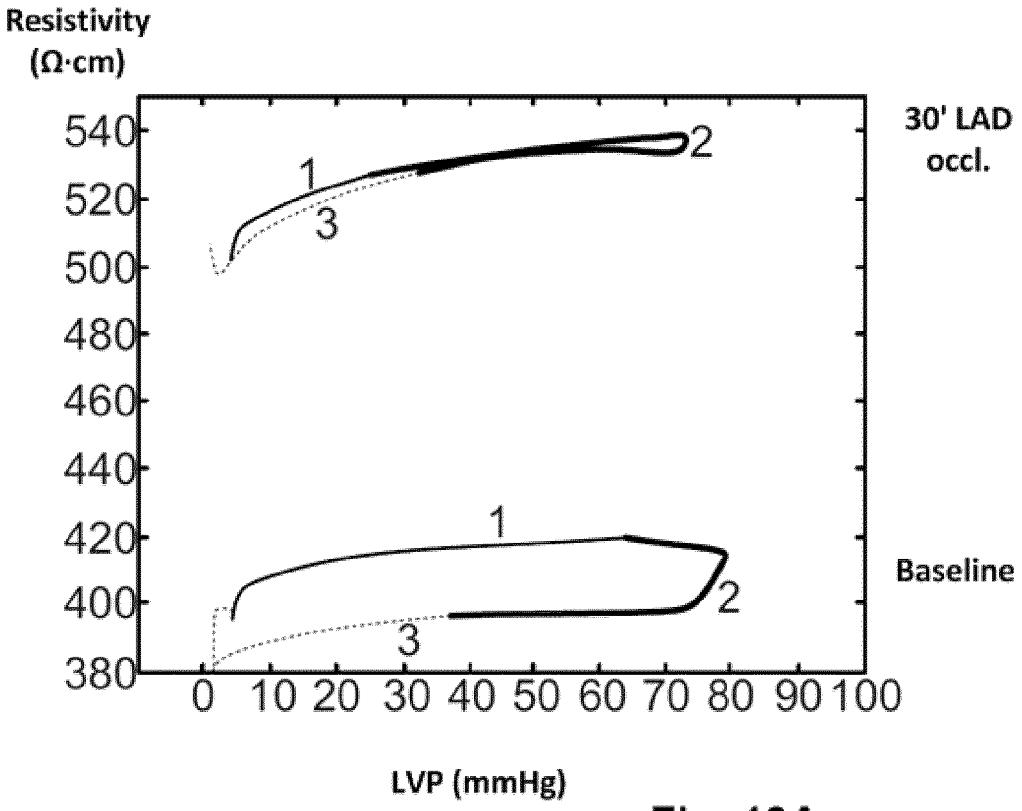

Fig. 13A

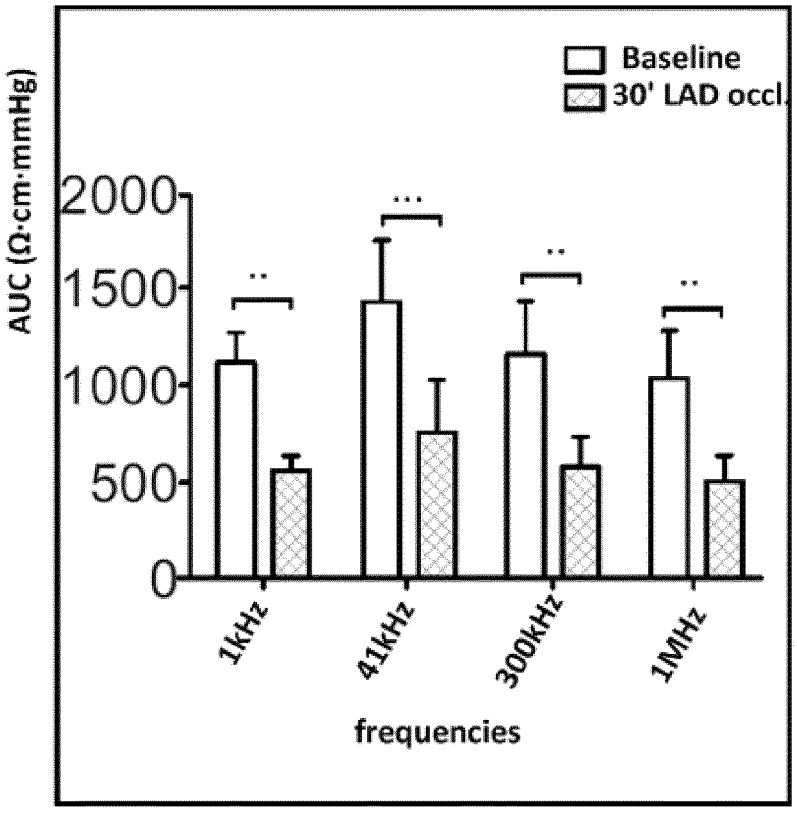

Fig. 13B

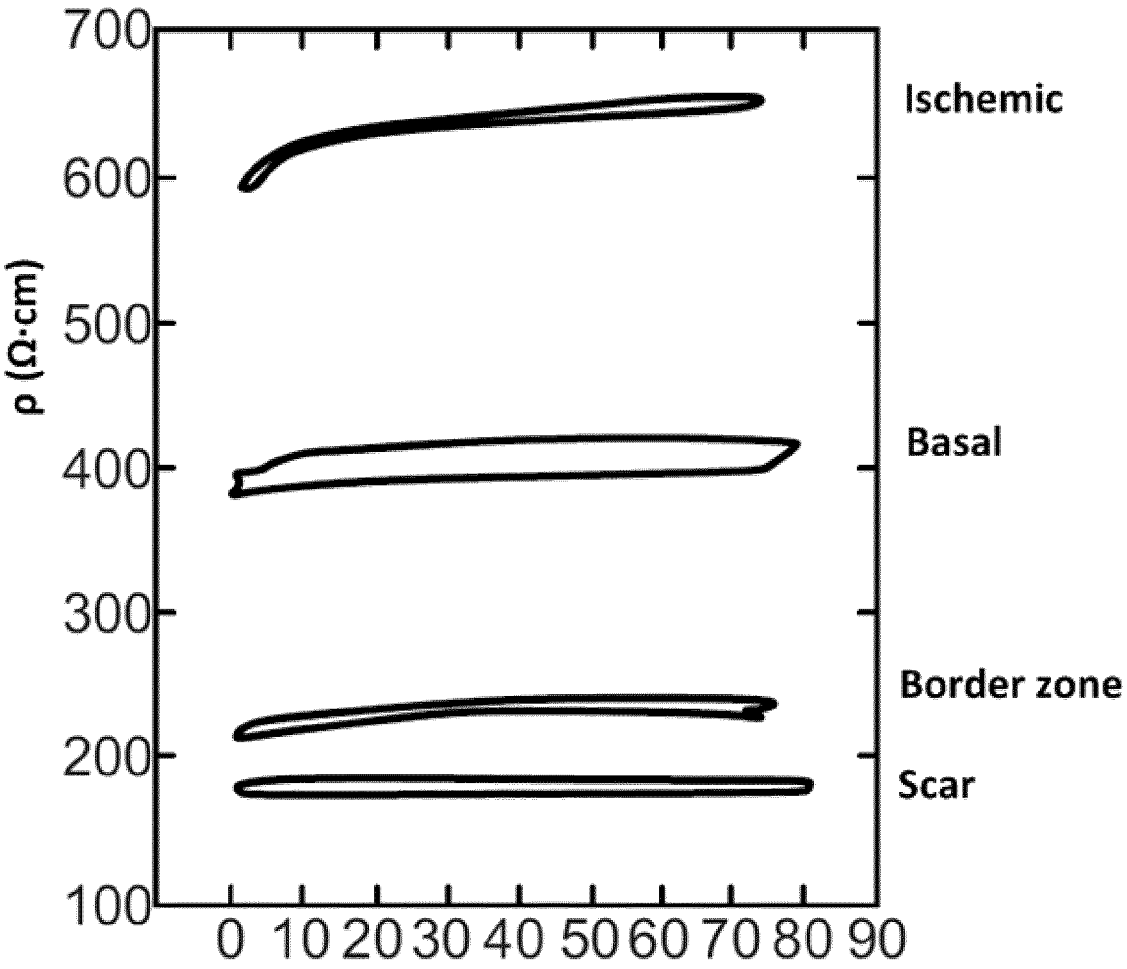
700
600
500
400
300
200
100
ρ (Ω·cm)
0 10 20 30 40 50 60 70 80 90
Ischemic
Basal
Border zone
Scar

Fig. 14

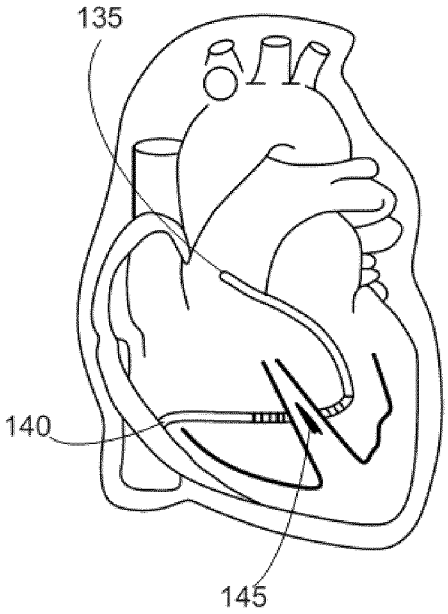

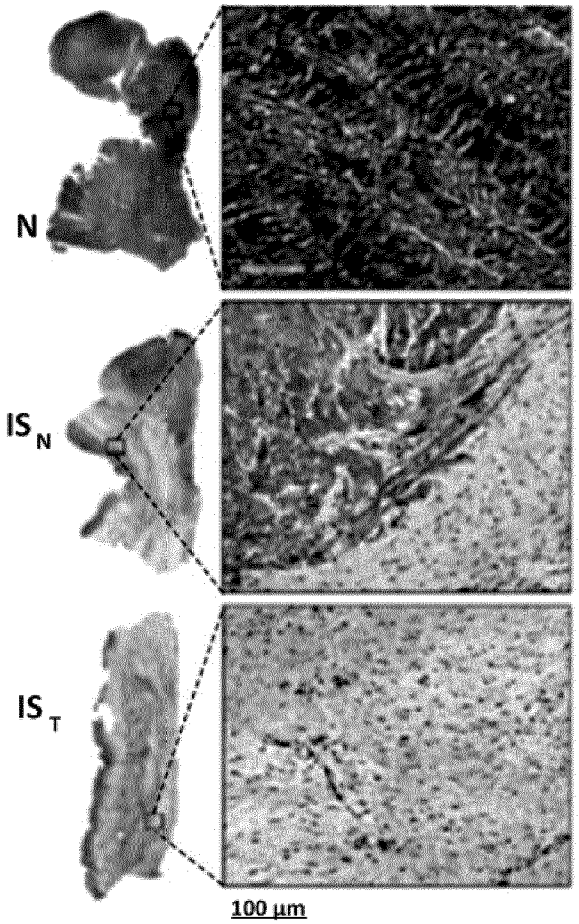

Fig. 15

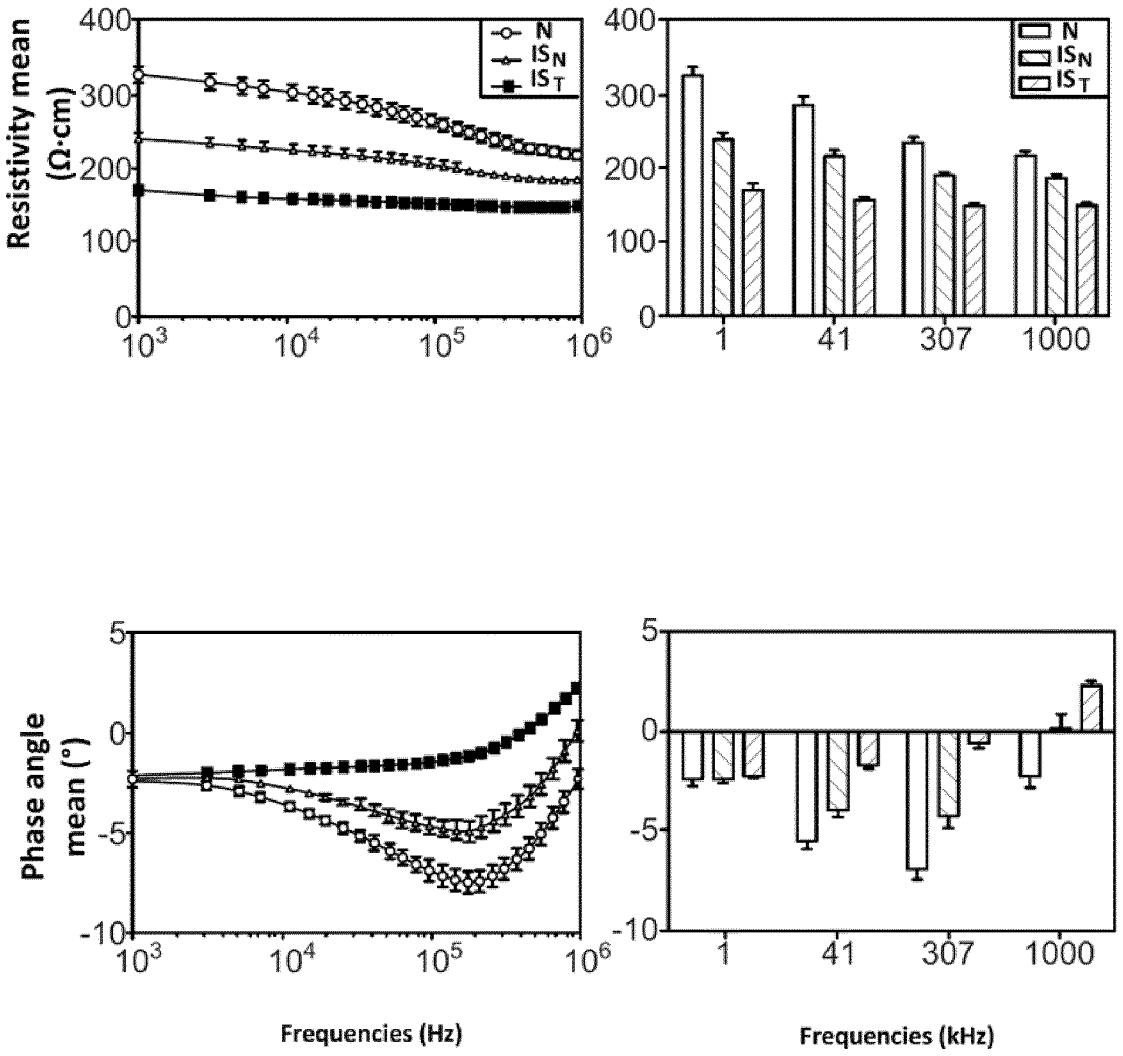

Fig. 16A

Fig. 16B

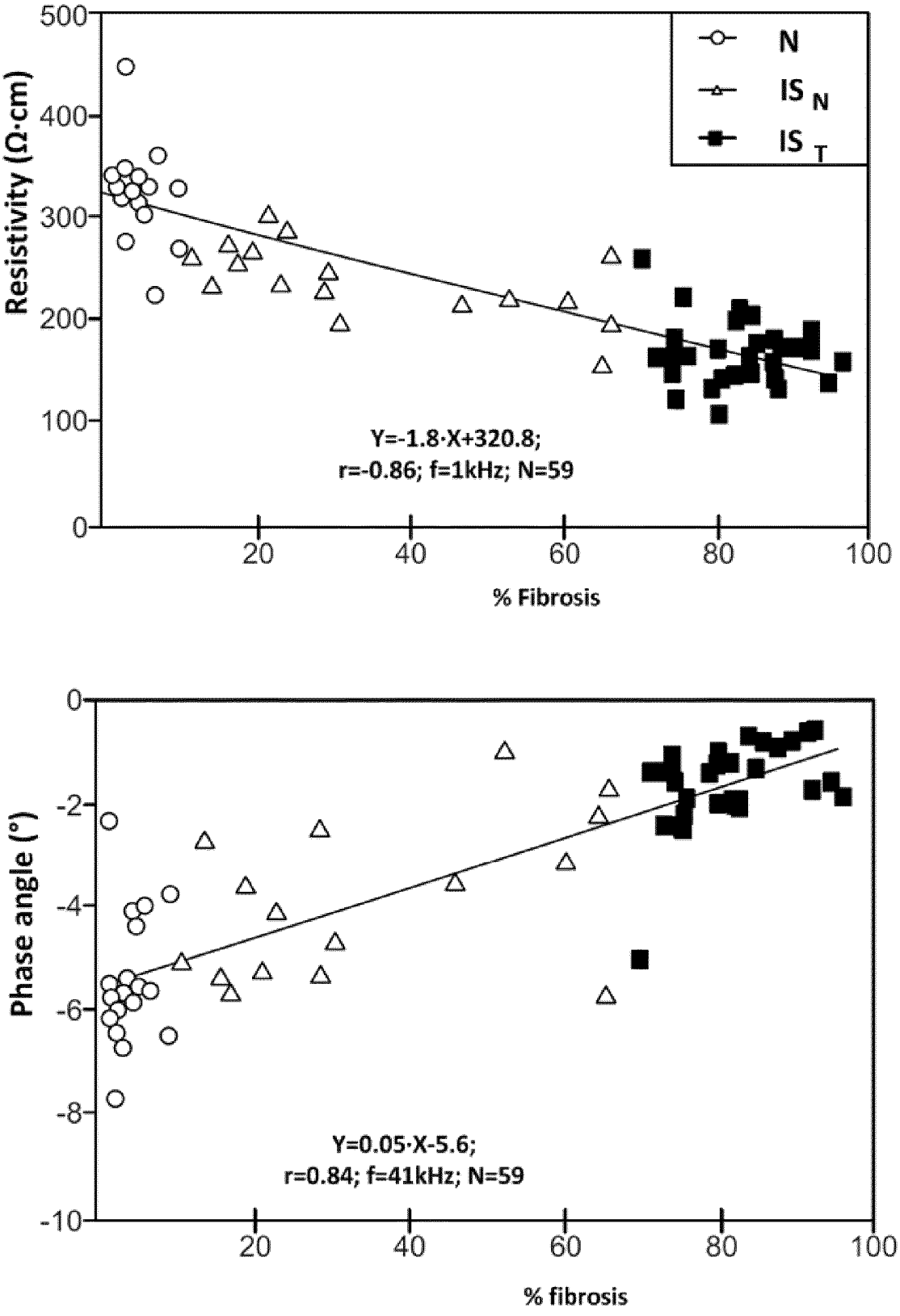
Resistivity (Ω·cm)
500
400
300
200
100
0
20
40
60
80
100
% Fibrosis
N
IS N
IS T
Y=-1.8·X+320.8;
r=-0.86; f=1kHz; N=59
Phase angle (°)
0
-2
-4
-6
-8
-10
20
40
60
80
100
% fibrosis
Y=0.05·X-5.6;
r=0.84; f=41kHz; N=59

Fig. 17

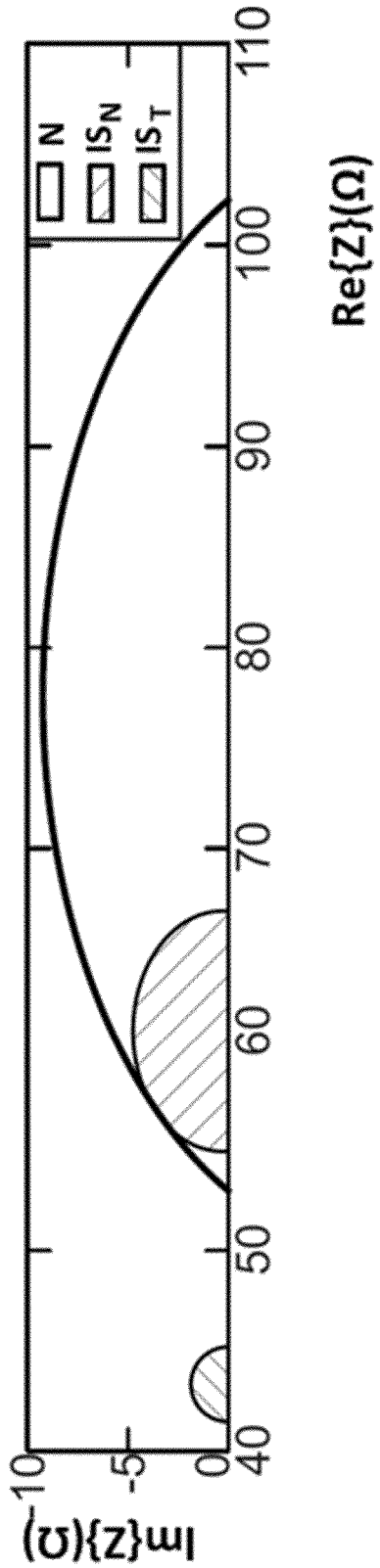

Fig. 18

Fig. 19A Fig. 19B Fig. 19C

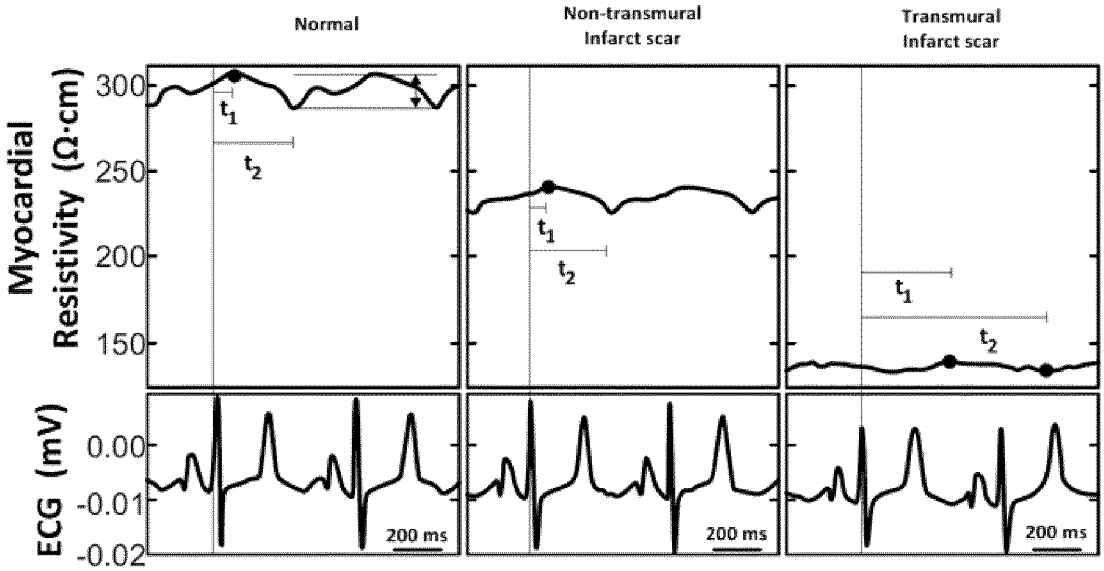

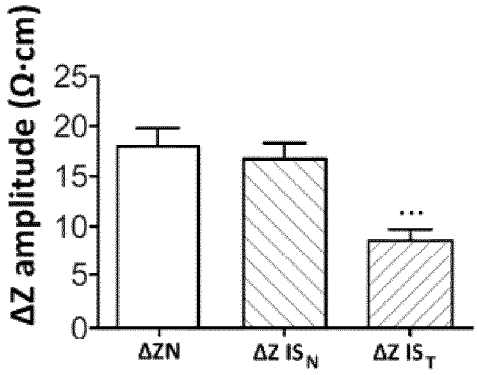

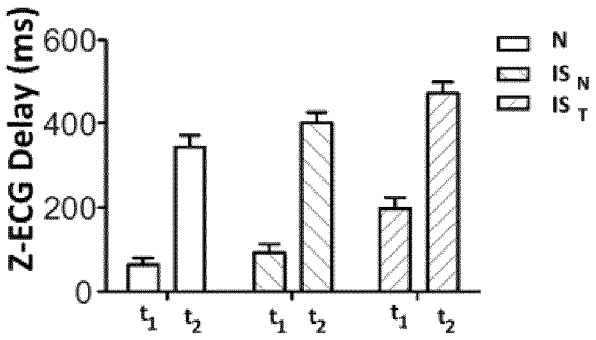

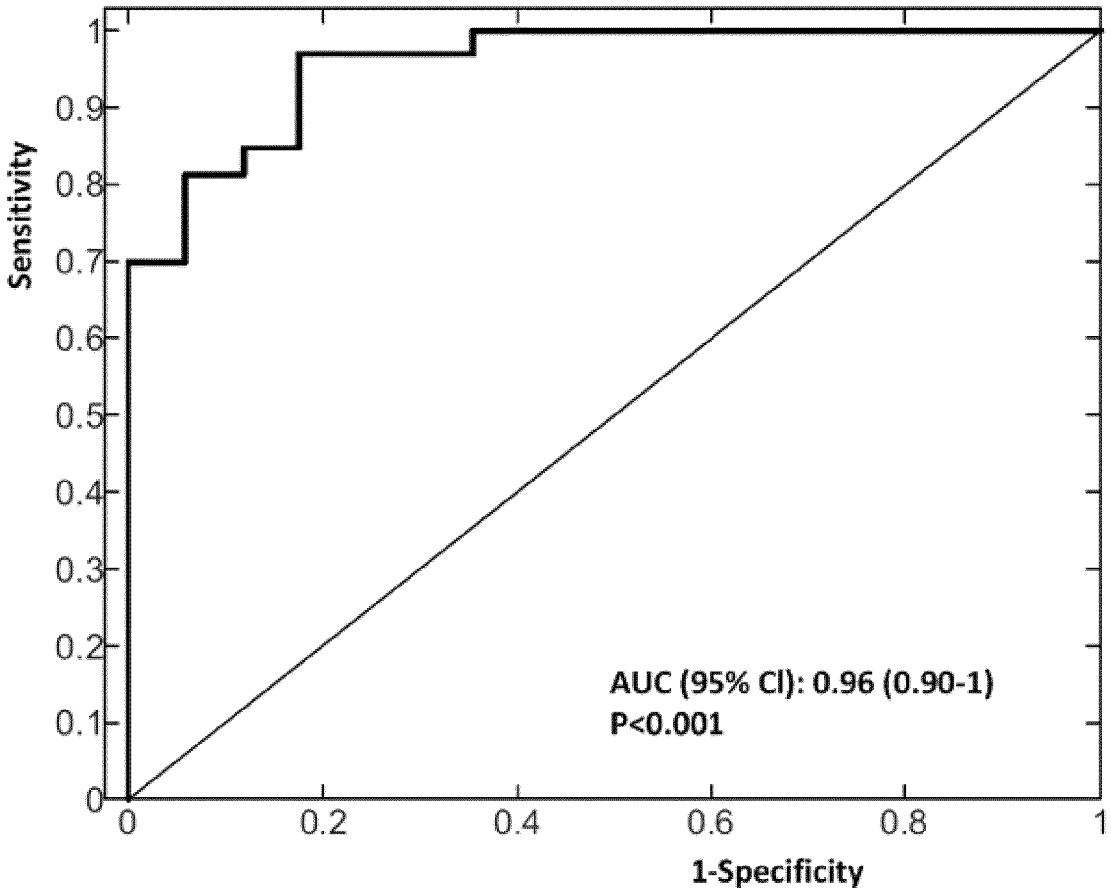
Sensitivity
1
0.9
0.8
0.7
0.6
0.5
0.4
0.3
0.2
0.1
0
0
0.2
0.4
0.6
0.8
1
1-Specificity
AUC (95% CI): 0.96 (0.90-1)
P<0.001

Fig. 20

	Excitation frequency (kHz)	r	p
Myocardial resistivity	1	-0.86	<0.001
	41	-0.85	<0.001
	307	-0.82	<0.001
	1 000	-0.76	<0.001
Phase angle	1	-0.19	=015
	41	-0.84	<0.001
	307	-0.83	<0.001
	1 000	-0.67	<0.001

TABLE 1

Sample region	R_0 (Ω)	R_{in}(Ω)	α	f_c (Hz)
Normal	1015±4.0	63.5±2.0	0.51±0.002	102.4±8.6
Non-transmural infarct scar	74.3±2.7"'	56.4±1.9'	0.30±0.03"'	80.9±10.9
Transmural infarct scar	53.7±2.0"'	46.8±15"'	0.24±0.03"'	17.3±3.2"'

TABLE 2

Parameter/s	ROC AUC (95%CI)	P
Mean resistivity	0.92 (0.83-1)	<0.001
Mean phase angle	0.91 (0.80-1)	<0.001
Phasic resistivity amplitude	0.83 (0.71-0.96)	<0.001
t_i interval	0.74 (0.58-0.89)	<0.01
Cole model		
P_o	0.91 (0.81-1)	<0.001
R_d	0.80 (0.66-0.94)	<0.001
f_c	0.95 (0.88-1)	<0.001
Resistivity + f_c	0.96 (0.90-1)	<0.001

TABLE 3

INTERNATIONAL SEARCH REPORT

International application No
PCT/EP2016/056933

A. CLASSIFICATION OF SUBJECT MATTER
INV. A61B5/053 A61B5/0452 A61B5/042 A61B5/0215 A61B5/029
A61N1/05 A61B5/00
ADD. A61B5/02 A61B5/107 A61B5/046 A61B5/0464 A61M25/00
According to International Patent Classification (IPC) or to both national classification and IPC

B. FIELDS SEARCHED

Minimum documentation searched (classification system followed by classification symbols)
A61B

Documentation searched other than minimum documentation to the extent that such documents are included in the fields searched

Electronic data base consulted during the international search (name of data base and, where practicable, search terms used)
EPO-Internal, WPI Data

C. DOCUMENTS CONSIDERED TO BE RELEVANT

Category*	Citation of document, with indication, where appropriate, of the relevant passages	Relevant to claim No.
X	ESTHER JORGE ED - MITAL R ET AL: "Early detection of acute transmural myocardial ischemia by the phasic systolic-diastolic changes of local tissue electrical impedance", AMERICAN JOURNAL OF PHYSIOLOGY, AMERICAN PHYSIOLOGICAL SOCIETY, USA, vol. 310, no. 3, 25 November 2015 (2015-11-25), pages H436-H443, XP008182498, ISSN: 1522-1539, DOI: 10.1152/AJPHEART.00754.2015 figures 1-4 page H436, right-hand column, paragraph 2 page H437, left-hand column, paragraphs 1, 2 page H437, right-hand column, paragraph 1 page H438, left-hand column, paragraph 2 page H443, left-hand column, paragraph 2 -/--	20-57

[X] Further documents are listed in the continuation of Box C.

[X] See patent family annex.

* Special categories of cited documents :

"A" document defining the general state of the art which is not considered to be of particular relevance

"E" earlier application or patent but published on or after the international filing date

"L" document which may throw doubts on priority claim(s) or which is cited to establish the publication date of another citation or other special reason (as specified)

"O" document referring to an oral disclosure, use, exhibition or other means

"P" document published prior to the international filing date but later than the priority date claimed

"T" later document published after the international filing date or priority date and not in conflict with the application but cited to understand the principle or theory underlying the invention

"X" document of particular relevance; the claimed invention cannot be considered novel or cannot be considered to involve an inventive step when the document is taken alone

"Y" document of particular relevance; the claimed invention cannot be considered to involve an inventive step when the document is combined with one or more other such documents, such combination being obvious to a person skilled in the art

"&" document member of the same patent family

Date of the actual completion of the international search	Date of mailing of the international search report
6 December 2016	19/12/2016

Name and mailing address of the ISA/	Authorized officer
European Patent Office, P.B. 5818 Patentlaan 2 NL - 2280 HV Rijswijk Tel. (+31-70) 340-2040, Fax: (+31-70) 340-3016	Meyer, Wolfgang

1

Form PCT/ISA/210 (second sheet) (April 2005)

C(Continuation). DOCUMENTS CONSIDERED TO BE RELEVANT

Category*	Citation of document, with indication, where appropriate, of the relevant passages	Relevant to claim No.
X	WO 2008/105691 A1 (ST JUDE MEDICAL [SE]; NORLIN ANNA [SE]; HENRIQUEZ LEDA [SE]; STRANDERB) 4 September 2008 (2008-09-04) page 2, lines 31, 32 page 12, line 24 page 23, line 30 page 27, lines 20,21 figures 1, 3a, 3b	20-23, 25,26, 29-34, 36-39
A	POLLARD ANDREW E ET AL: "A New Approach for Resolution of Complex Tissue Impedance Spectra in Hearts", IEEE TRANSACTIONS ON BIOMEDICAL ENGINEERING, IEEE SERVICE CENTER, PISCATAWAY, NJ, USA, vol. 60, no. 9, 1 September 2013 (2013-09-01), pages 2494-2503, XP011524033, ISSN: 0018-9294, DOI: 10.1109/TBME.2013.2258917 [retrieved on 2013-08-16] page 2499, right-hand column, last paragraph - page 2500, left-hand column, paragraph first	21
A	Y. SALAZAR ET AL: "Transmural Versus Nontransmural In Situ Electrical Impedance Spectrum for Healthy, Ischemic, and Healed Myocardium", IEEE TRANSACTIONS ON BIOMEDICAL ENGINEERING., vol. 51, no. 8, 1 August 2004 (2004-08-01) , pages 1421-1427, XP055324987, PISCATAWAY, NJ, USA. ISSN: 0018-9294, DOI: 10.1109/TBME.2004.828030 tables I, II	26,29
A	US 2004/260278 A1 (ANDERSON SCOTT C [US] ET AL) 23 December 2004 (2004-12-23) paragraphs [0101], [0115], [0135], [0151], [0161], [0167] figures 2A-2F	32, 41-49, 52-54

-/--

C(Continuation). DOCUMENTS CONSIDERED TO BE RELEVANT

Category*	Citation of document, with indication, where appropriate, of the relevant passages	Relevant to claim No.
A	SANCHEZ B ET AL: "Novel Estimation of the Electrical Bioimpedance Using the Local Polynomial Method. Application to In Vivo Real-Time Myocardium Tissue Impedance Characterization During the Cardiac Cycle", IEEE TRANSACTIONS ON BIOMEDICAL ENGINEERING, IEEE SERVICE CENTER, PISCATAWAY, NJ, USA, vol. 58, no. 12, 1 December 2011 (2011-12-01), pages 3376-3385, XP011408580, ISSN: 0018-9294, DOI: 10.1109/TBME.2011.2166116 chapter "C. Algorithm" equation (20) figure 11	33,34
A	US 2010/204585 A1 (ZHANG HONGXUAN [US]) 12 August 2010 (2010-08-12) paragraphs [0020] - [0022] figures 2, 3	36,37
A	US 2007/191901 A1 (SCHECTER STUART O [US]) 16 August 2007 (2007-08-16) paragraphs [0119] - [0121] figures 6a, 8, 9	38,39
A	WO 2014/008489 A1 (CIBIEM INC [US]) 9 January 2014 (2014-01-09) the whole document	20-57
A	US 2011/144510 A1 (RYU KYUNGMOO [US] ET AL) 16 June 2011 (2011-06-16) the whole document	20-57
A	BRAGOS R ET AL: "Characterisation of dynamic biologic systems using multisine based impedance spectroscopy", IMTC 2001. PROCEEDINGS OF THE 18TH. IEEE INSTRUMENTATION AND MEASUREMENT TECHNOLOGY CONFERENCE. BUDAPEST, HUNGARY, MAY 21 - 23, 2001; [IEEE INSTRUMENTATION AND MEASUREMENT TECHNOLOGY CONFERENCE. (IMTC):], NEW YORK, NY : IEEE, US, vol. 1, 21 May 2001 (2001-05-21), pages 44-47, XP010546659, DOI: 10.1109/IMTC.2001.928785 ISBN: 978-0-7803-6646-6 the whole document	20-57
A	US 2006/184060 A1 (BELALCAZAR ANDRES [US] ET AL) 17 August 2006 (2006-08-17) the whole document	20-57

1

INTERNATIONAL SEARCH REPORT

International application No.
PCT/EP2016/056933

Box No. II Observations where certain claims were found unsearchable (Continuation of item 2 of first sheet)

This international search report has not been established in respect of certain claims under Article 17(2)(a) for the following reasons:

1. [X] Claims Nos.: 1-19
because they relate to subject matter not required to be searched by this Authority, namely:

The present application does not meet the requirements of Rule 39.1(iv) because claims 1-19 are comprising a method for treatment of the human body by surgery. Particularly, placement and re-placement of a catheter on an area of a cardiac tissue is a surgical step.

2. [ ] Claims Nos.:
because they relate to parts of the international application that do not comply with the prescribed requirements to such an extent that no meaningful international search can be carried out, specifically:

3. [ ] Claims Nos.:
because they are dependent claims and are not drafted in accordance with the second and third sentences of Rule 6.4(a).

Box No. III Observations where unity of invention is lacking (Continuation of item 3 of first sheet)

This International Searching Authority found multiple inventions in this international application, as follows:

1. [ ] As all required additional search fees were timely paid by the applicant, this international search report covers all searchable claims.

2. [ ] As all searchable claims could be searched without effort justifying an additional fees, this Authority did not invite payment of additional fees.

3. [ ] As only some of the required additional search fees were timely paid by the applicant, this international search report covers only those claims for which fees were paid, specifically claims Nos.:

4. [ ] No required additional search fees were timely paid by the applicant. Consequently, this international search report is restricted to the invention first mentioned in the claims; it is covered by claims Nos.:

Remark on Protest

[ ] The additional search fees were accompanied by the applicant's protest and, where applicable, the payment of a protest fee.

[ ] The additional search fees were accompanied by the applicant's protest but the applicable protest fee was not paid within the time limit specified in the invitation.

[ ] No protest accompanied the payment of additional search fees.

INTERNATIONAL SEARCH REPORT

Information on patent family members

International application No
PCT/EP2016/056933

Patent document cited in search report	Publication date	Patent family member(s)	Publication date
WO 2008105691 A1	04-09-2008	EP 2114526 A1	11-11-2009
		US 2010280563 A1	04-11-2010
		WO 2008105691 A1	04-09-2008
US 2004260278 A1	23-12-2004	NONE	
US 2010204585 A1	12-08-2010	NONE	
US 2007191901 A1	16-08-2007	NONE	
WO 2014008489 A1	09-01-2014	CN 104755010 A	01-07-2015
		EP 2869751 A1	13-05-2015
		US 2014018788 A1	16-01-2014
		WO 2014008489 A1	09-01-2014
US 2011144510 A1	16-06-2011	NONE	
US 2006184060 A1	17-08-2006	CN 101163443 A	16-04-2008
		EP 1848334 A2	31-10-2007
		HK 1119550 A1	15-10-2010
		JP 2008529678 A	07-08-2008
		US 2006184060 A1	17-08-2006
		WO 2006088805 A2	24-08-2006

专利名称(译)	通过测量心动周期期间的电阻抗来评估梗塞心肌组织的系统和方法		
公开(公告)号	EP3435858A1	公开(公告)日	2019-02-06
申请号	EP2016712341	申请日	2016-03-30
[标]申请(专利权)人(译)	加泰罗尼亚理工大学 FUNDACIO INSTITUT DE RECERCA DE LHOSPITAL DE LA圣克鲁我的Sant Pau		
申请(专利权)人(译)	Universität大学POLITÈCNICADE CATALUNYA fundacio所recerca L'Hospital de la Santa认为i Sant棒		
当前申请(专利权)人(译)	Universität大学POLITÈCNICADE CATALUNYA fundacio所recerca L'Hospital de la Santa认为i Sant棒		
[标]发明人	ROSELL FERRER FRANCESC XAVIER CINCA CUSCULLOLA JUAN BRAGOS BARDIA RAMON AMOROS FIGUERAS GERARD JORGE VIZUETE ESTHER GARCIA SANCHEZ TOMAS SANCHEZ TERRONES BENJAMIN		
发明人	ROSELL FERRER, FRANCESC XAVIER CINCA CUSCULLOLA, JUAN BRAGÓS BARDIA, RAMÓN AMORÓS FIGUERAS, GERARD JORGE VIZUETE, ESTHER GARCÍA SÁNCHEZ, TOMÀS SÁNCHEZ TERRONES, BENJAMÍN		
IPC分类号	A61B5/053 A61B5/0452 A61B5/042 A61B5/0215 A61B5/029 A61N1/05 A61B5/00 A61B5/02 A61B5/107 A61B5/046 A61B5/0464 A61M25/00 A61B5/06		
CPC分类号	A61B5/02007 A61B5/0215 A61B5/029 A61B5/0422 A61B5/0452 A61B5/046 A61B5/0464 A61B5/0538 A61B5/061 A61B5/107 A61B5/6852 A61B2505/05 A61B18/1492		
其他公开文献	EP3435858B1		
外部链接	Espacenet		

摘要(译)

本文公开了用于识别梗塞组织（例如慢性心肌梗塞组织）的范围和深度的方法和装置。本发明适用于心脏组织，但也可用于评估其他器官中的瘢痕过程。该方法的示例包括以频率宽带注入交流电脉冲，同时连续地（以非常高的采样率）测量电压信号以在整个心动周期期间获得电阻抗（Z(f,t)）。可以使用腔内电导管进行阻抗测量。